AD-A074 751 DOUGLAS AIRCRAFT CO LONG BEACH CA F/G 20/4
A HIGHER ORDER PANEL METHOD FOR THREE-DIMENSIONAL POTENTIAL FLO--ETC(U)
JUN 79 J L HESS N62269-77-C-0437
UNCLASSIFIED MDC-J8519 NADC-77166-30 NL

1 OF 1
AD A074751

END
DATE FILMED
11-79
DDC

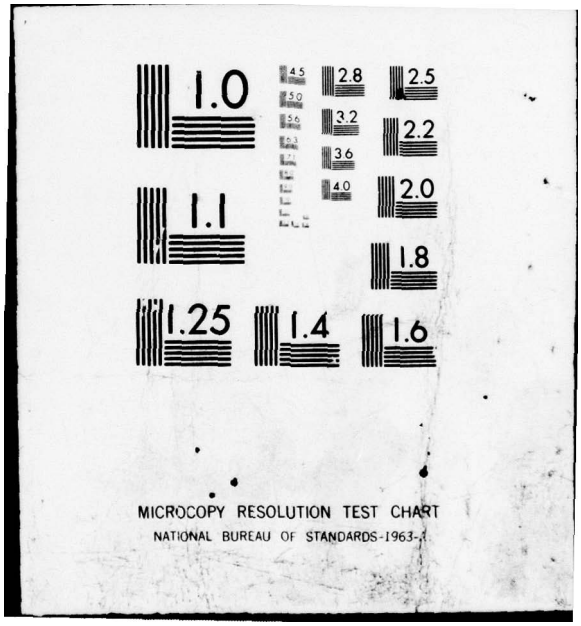
1.0
1.1
1.25
1.4
1.6
1.8
2.0
2.2
2.5
2.8
3.2
3.6
4.0
4.5
5.0
5.6
MICROCOPY RESOLUTION TEST CHART
NATIONAL BUREAU OF STANDARDS-1963-A

(12)

Report No. NADC 77166-30

Report No. MDC J8519

LEVEL II

A HIGHER ORDER PANEL METHOD FOR THREE-DIMENSIONAL POTENTIAL FLOW

by

John L. Hess

June 1979

prepared under

Contract No. N62269-77-C-0437

for

Naval Air Development Center

Warminster, Penn.

Report No. NADC 77166-30

Report No. MDC J8519

A HIGHER ORDER PANEL METHOD FOR THREE-DIMENSIONAL POTENTIAL FLOW

by

John L. Hess

June 1979

prepared under
Contract No. N62269-77-C-0437

for

Naval Air Development Center
Warminster, Penn.

Unclassified

SECURITY CLASSIFICATION OF THIS PAGE (When Data Entered)

REPORT DOCUMENTATION PAGE	READ INSTRUCTIONS BEFORE COMPLETING FORM
1. REPORT NUMBER: NADC 77166-30	2. GOVT ACCESSION NO.
3. RECIPIENT'S CATALOG NUMBER	
4. TITLE (and Subtitle): A Higher Order Panel Method for Three-Dimensional Potential Flow.	5. TYPE OF REPORT & PERIOD COVERED: Final Report.
6. PERFORMING ORG. REPORT NUMBER: MDC-J8519	
7. AUTHOR(s): John L. Hess	8. CONTRACT OR GRANT NUMBER(s): N62269-77-C-0437
9. PERFORMING ORGANIZATION NAME AND ADDRESS: Douglas Aircraft Company, 3855 Lakewood Blvd, Long Beach, CA 90846	10. PROGRAM ELEMENT, PROJECT, TASK AREA & WORK UNIT NUMBERS: 62 86
11. CONTROLLING OFFICE NAME AND ADDRESS: Naval Air Development Center, Warminster, PA 18974 6053	12. REPORT DATE: June 1979
	13. NUMBER OF PAGES: 85
14. MONITORING AGENCY NAME & ADDRESS (if different from Controlling Office)	15. SECURITY CLASS. (of this report): Unclassified
	15a. DECLASSIFICATION/DOWNGRADING SCHEDULE

16. DISTRIBUTION STATEMENT (of this Report)

Approved for public release; distribution unlimited

17. DISTRIBUTION STATEMENT (of the abstract entered in Block 20, if different from Report)

18. SUPPLEMENTARY NOTES

19. KEY WORDS (Continue on reverse side if necessary and identify by block number)

Aerodynamics	Higher Order	Source Density
Computer Program	Numerical Analysis	Surface Singularity
Flow Field	Panel Method	Three-Dimensional Flow
Fluid Dynamics	Potential Flow	

20. ABSTRACT (Continue on reverse side if necessary and identify by block number)

The method described here is a higher-order three-dimensional surface panel method. It utilizes four-sided panels on the actual surface of the body about which flow is to be computed and is thus applicable to arbitrary configurations. In contrast to a first-order panel method that uses flat panels, usually with constant source and/or vorticity density, the present method uses curved panels of second degree with linearly varying source and vorticity density. The mathematical problem solved is that of incompressible potential flow, but the

DD FORM 1 JAN 73 1473 EDITION OF 1 NOV 65 IS OBSOLETE S/N 0102-014-6601

Unclassified 116 400

SECURITY CLASSIFICATION OF THIS PAGE (When Data Entered)

calculation can be extended to subsonic flow by means of well-known compressibility corrections.

This report presents a discussion of the techniques adopted and some alternatives. A rigorous derivation of the higher-order formulation is carried out. All formulas and logic required by the method are included, except that the report on the corresponding first-order method is relied on for formulas and procedures common to the two techniques. First-order and higher-order calculated results are compared with each other and with exact solutions.

Copy number

Report number MDC J8519

A HIGHER ORDER PANEL METHOD FOR THREE-DIMENSIONAL POTENTIAL FLOW

Revision date

Revision letter

Issue date June 1979

Contract number N62269-77-C-0437

Prepared by: John L. Hess

Approved by:

Tuncer Cebeci
Chief Technology Engineer
Research
Aerodynamics Subdivision

Frank T. Lynch
Branch Chief
Research and Development
Aerodynamics Subdivision

R. B. Harris
Director — Aerodynamics

DOUGLAS AIRCRAFT COMPANY
MCDONNELL DOUGLAS CORPORATION

1.0 ABSTRACT

The method described here is a higher-order three-dimensional surface panel method. It utilizes four-sided panels on the actual surface of the body about which flow is to be computed and is thus applicable to arbitrary configurations. In contrast to a first-order panel method that uses flat panels, usually with constant source and/or vorticity density, the present method uses curved panels of second degree with linearly varying source and vorticity density. The mathematical problem solved is that of incompressible potential flow, but the calculation can be extended to subsonic flow by means of well-known compressibility corrections.

This report presents a discussion of the techniques adopted and some alternatives. A rigorous derivation of the higher-order formulation is carried out. All formulas and logic required by the method are included, except that the report on the corresponding first-order method is relied on for formulas and procedures common to the two techniques. First-order and higher-order calculated results are compared with each other and with exact solutions.

2.0 TABLE OF CONTENTS

3.0 INTRODUCTION

Recent years have witnessed the acceptance of so-called "panel methods" for calculating three-dimensional potential flows to such an extent that they are now considered to be routine tools of aerodynamic and hydrodynamic design. While some supersonic work has been done, by far the chief emphasis in panel method development has been directed to the solution of Laplace's equation for incompressible flow. The results obtained are generalized to subsonic flows by the application of certain compressibility corrections. Panel methods may be grouped into two broad categories. Surface panel methods place panels and satisfy normal velocity boundary conditions on the surface of the body about which flow is to be computed. (Actually the numerical surface is a close approximation to the body surface, which it approaches in the limit of infinite panel number.) This type of panel method is unrestricted, and exact in the sense that it is applicable to completely arbitrary bodies and that incompressible flow may be calculated to any degree of precision by increasing the panel number. On the contrary, mean-surface panel methods place panels interior to the body in question, e.g., on the axis of a body of revolution or on the mean surface of a wing. This type of panel method is approximate and is applicable to slender bodies, and to cases where the flow perturbation velocities are small. Both types of method have their uses. Mean-surface panel methods are used for preliminary design, while surface panel methods are used for final detailed calculations. It is with incompressible surface panel methods that the present report is concerned.

Panel methods arise as numerical discretizations of the theoretical technique that may be denoted the surface singularity approach. In this procedure the surface of the body about which flow is to be computed is imagined to be covered with distributions of flow singularity: source, dipole, vorticity, and the variable strengths of these distributions are adjusted to satisfy the normal velocity boundary condition on the body surface and any auxiliary conditions, such as Kutta conditions along a wing trailing edge. In particular the normal velocity boundary condition leads to an integral equation in the singularity strengths. In the numerical implementation of this technique the first step must be to discretize the body surface. In three-dimensional problems the body surface is represented by a large number

of small four-sided surface elements or "panels" which is the origin of the name "panel methods."

There are various possibilities for distributing types of singularities on the surface panels and different investigators have made different choices for their methods. However, it is common to all methods that one particular type of singularity is assigned primary responsibility for satisfying the normal velocity boundary condition and thus may be called the basic singularity. Other types of singularity have primary responsibility for auxiliary conditions and may be called auxiliary singularities. (Clearly all conditions must ultimately be satisfied simultaneously but the above is a valid distinction.) It has become customary to categorize a panel method according to its basic singularity. Thus, reference is made to source methods, dipole methods, and vortex methods. This report is concerned with generalizations of the Hess panel method (refs. 1 and 2), which is in such common use throughout the country that it may fairly be called the standard existing procedure. The Hess technique is a source method, and the descriptions below apply to that type of method, although parallel descriptions for the other methods would differ only in detail.

The panel-method representation of a three-dimensional body is shown in figure 1. On each panel a control point is selected where the boundary condition of zero normal velocity is to be applied and where surface velocities are ultimately calculated. A "matrix of influence coefficients" is then calculated. This consists of the complete set of velocities induced by the panels at each others' control points for certain nominal variations of the singularity strengths, e.g., constant at unit value, linearly varying with unit derivative, etc. On nonlifting portions of the configuration (figure 1) only source singularity is employed. On lifting portions both source and either dipole or vorticity singularities are used. It can be shown (ref. 1) that surface distributions of dipole and of vorticity are equivalent. The dipole has been used most commonly in three dimensions because it is a scalar rather than a vector and because it automatically satisfies the appropriate conservation theorems that must be applied to vorticity distributions (essentially, zero divergence of vorticity). From the basic standpoint a lifting portion of the configuration is defined as one having a sharp trailing edge where a Kutta condition is to be applied and from which issues a wake of trailing vorticity

(figure 1). Nonlifting portions are characterized by the absence of a trailing edge and its associated vortex wake. The prototypes of lifting and nonlifting portions are a wing and a fuselage, respectively. On the wake only dipole (vorticity) singularity is needed. However, from the panel-method standpoint there is a change of emphasis. A lifting portion is characterized by one having bound vorticity whose strength is adjusted to satisfy certain conditions, while a nonlifting portion has no vorticity and no conditions.

A panel method approximates the integral equation that expresses the zero normal-velocity boundary condition by a set of linear algebraic equations for the values of singularity strengths on the panels. In lifting cases the Kutta condition along the trailing edge (figure 1) yields a small number of additional equations. On each panel one point, which is designated the control point, is selected, and the normal velocity is required to be zero there. Each panel has an independent value of source strength. This provides a number of unknown parameters equal to the number of panels and, more particularly equal to the number of linear equations expressing the condition of zero normal velocity. The Kutta condition is discretized by applying it at a finite number of locations along the trailing edge. The dipole (vorticity) distribution over the surface is then specialized to be expressible in terms of a number of adjustable parameters equal to the number of locations at which the Kutta condition is applied. Once this has been accomplished, there are the same number of unknown values of singularity as there are conditions to be satisfied. In nonlifting flows, no Kutta condition is applied, and the source strengths are calculated to yield zero normal velocity at the control points. This summary is necessarily brief. Details are contained in references 1 and 2.

In the standard form of the Hess panel method in both its nonlifting (ref. 2) and lifting (ref. 1) versions, the surface panels of figure 1 are plane quadrilaterals and the source strength on each panel is assumed constant — a step function from element to element. (The dipole variation, however, is more elaborate, (ref. 1).) This standard, which is referred to as the base method, has proved satisfactory in numerous applications by investigators in industry, government, and academia. However, experience has indicated that certain improvements would be desirable. Probably the principal disadvantage of the Hess method or any three-dimensional panel method is that each case is relatively expensive. This expense consists of two parts:

the human labor necessary to prepare the rather large amount of input data and the computer cost required to carry out the calculations. Ironically, the problem of computing time has been intensified by the very success of the method in application. Namely, its success has led to its use in more and more challenging problems. The result is that some of the most frequent users of the method have found themselves employing ever larger numbers of surface panels to represent complicated configurations accurately. This trend has been in evidence for some time. For a long while, the largest panel number used was 1000. However, recent experience has greatly increased this number. The largest case run to date employed 3500 surface panels on each half of the configuration (symmetry was employed so that the order of the influence matrix was 3500). Computing time for a panel method increases as the square of the panel number or faster. (If a direct solution of the linear equations is used, the time can vary as the cube of the panel number.) Thus large panel numbers require very long computation times and thus very large costs. Moreover, the accuracies obtained are not always what is desired. Accordingly, there is a need for an increase in speed of computation with no decrease in accuracy, or better still, with an increase in accuracy. This has been the aim of the work described in this report.

To reduce the other major expense, i.e., the man-hours required for inputting a body to a panel method, a so-called "geometry package" has been constructed (refs. 3 and 4). This routine, which is a major program in its own right, enables a user of the method to input a relatively small number of points defining his particular body. Moreover, relatively little care will be required in selecting the particular points to input. The "geometry package" will then enrich the point number, redistribute the points as needed according to one of a number of algorithms, compute intersections of various portions of the configuration, etc. For certain frequently-occurring cases the procedure will be completely automatic. For others, there will still be a "man in the loop," but his labor will be greatly reduced. Figure 2a shows a very sparse representation of a wing-fuselage that was input to the geometry package which then produced the enriched panelling of figure 2b. Included in the process is the calculation of the wing-fuselage intersection curve. This geometry package has been combined with the higher-order program of the present report.

Both logically and mathematically, the present method is an extension of the base method of reference 1. Indeed many formulas and procedures are common to the two programs. If the present report were to be made self-contained, it would have to contain a very large percentage of the material presented in reference 1. This would not only be repetitious but would make the present report extremely lengthy. Accordingly, it is assumed that a reader interested in details has reference 1 available, and reference is freely made to equations and sections of that report. However, it is possible to obtain a general familiarity with the present method without using reference 1.

4.0 GENERAL DESCRIPTION OF THE HIGHER-ORDER PANEL METHOD

The purpose of the work described in this report is to increase the speed and accuracy of the Hess panel method by use of a higher-order formulation. The higher-order formulation replaces the standard base method's assumption of plane surface panels having constant values of source strength (and a quadratic dipole strength) by an assumption of curved panels with variable source and dipole strength. A direct analogy of this approach has already been applied with great success to the two-dimensional case (ref. 5) and the axisymmetric case (ref. 6). The concept of the higher-order approach was first put forward in reference 5, where it was shown that the effect of surface curvature and the effect of the variation of surface singularity strength are of the same order of magnitude. Thus, inclusion of one without the other, as is done for instance by several investigators in two dimensions, is inconsistent and, in general, does not lead to an improvement in accuracy over the base method. Use of the consistent higher-order formulation has yielded large increases in both computational speed and accuracy for two-dimensional and axisymmetric flows (refs. 5, 6 and 7). The present three-dimensional higher-order formulation yields comparable gains in speed and accuracy.

Conceptually, the essence of constructing a higher-order panel method consists of generating an altered "matrix of influence coefficients" (previous section). All other aspects of the program, e.g., input of the body geometry, solution of the linear equations, calculation of surface velocities and pressures, remain the same. Specifically, the formulas that in the base method give the velocity induced at an arbitrary control point by a flat panel with a constant source strength must be replaced in a higher-order method by formulas that give the velocity induced at an arbitrary control point by a curved panel with a variable source strength. Similarly the formulas that in the base method give the velocity due to a quadratic dipole strength over a flat panel are replaced by those appropriate to a curved panel. Determination of the form of the panel shape and the variation of the singularity strength has been part of the problem. It turned out that derivation of new velocity formulas was only half the required task. A considerable amount of new logic was also required.

The starting point of the present work is the consistency analysis of reference 8, which considers a surface-source distribution. It is shown, therein, that consistent approximations in ascending order of accuracy are: (1) flat-panel constant-source (base method), (2) paraboloidal-panel linear-source, and (3) cubic-panel quadratic-source. In other words, a consistent approach always uses a source polynomial one degree less than the panel polynomial. Reference 8 also gives the form of the expansion and the number of basic integrals over the panel that are required by each order of approximation. Thus, the flat-panel constant-source approach requires a single integral. The paraboloidal-panel linear-source approach requires five additional integrals — a total of six. Finally, the cubic-panel quadratic-source approach requires a total of 23 integrals. This last is felt to be too complicated to be feasible and thus the "higher-order" procedure adopted is the paraboloidal-panel linear-source. This is the direct analogy of the formulation that proved so effective in the two-dimensional and axisymmetric cases (refs. 5 and 6). For completeness the expansions derived in reference 8 are presented in section 5.1, and thus the present report supercedes reference 8.

A second consistency analysis is necessary for the dipole or vorticity distribution required to produce lift. From specific two-dimensional formulas, as well as general three-dimensional considerations, it is expected that a consistent vorticity distribution has the same degree as the source distribution. Thus, according to the relation between dipole and vorticity distributions (ref. 1), the consistent dipole distribution has a degree one higher than that of the source distribution. However, when the analysis is performed for the integrated effect of a single panel, it turns out that the quadratic dipole terms are of the same order as cubic geometry terms (as is the case for the source distribution). This unfortunate behavior is due to the so-called "edge vortex." As derived in reference 1, a variable dipole distribution over a finite area is equivalent to the sum of a vorticity distribution over the area with strength equal to the gradient of the dipole strength plus a concentrated vortex filament around the edge of the area with variable strength equal to the local dipole strength. It is due to the edge vortex that the cubic geometry terms enter to a lower order than expected. Clearly the actual wing of figure 1 does not have concentrated vortices along panel edges. Their presence is due to the fact that formulas are derived for one isolated panel. The effects of the edge vortex on a panel are presumably cancelled by equal

and opposite edge-vortices on adjacent panels. If the geometry and the dipole strength are continuous across panel edges, this cancellation is exact. Otherwise it is approximate. However, the edge-vortex effects enter the basic expansion formulas in a way that makes it difficult to cancel them analytically.

The procedure adopted to avoid the above difficulty is the use of a vorticity distribution, rather than a dipole distribution, on a panel. Induced velocity formulas are derived from the surface analogy of the Biot-Savart Law, and the edge vortex is avoided. To insure that the vorticity conservation theorems are satisfied over the interior of a panel, the vector vorticity strength is expressed in terms of derivatives of an equivalent dipole strength. To the extent that edge vortices on adjacent panels do not completely cancel the velocity field produced by the sum of all panels is nonpotential, but this error is of order equal to other errors of the formulation. To insure this result, the nominal dipole strength must be nearly continuous across panel edges. This is always the case for adjacent panels in the same lifting strip of panels (figure 1). To obtain near continuity from strip to strip, i.e., across the N-lines, it is necessary to use the piecewise-linear spanwise vorticity variation rather than the piecewise constant option (ref. 1). Along physical edges of the body, such as sheared off wing tips, an edge vortex is "physically" required. Either physical edges require special formulas not incorporated into the initial version of the present method or special techniques for use of the method are needed to simulate edge effects. Clearly further study of this situation is required (section 5.3).

The principal analytic task of the present work consisted of deriving analytic expressions for the various integrals of section 5.0. It is important that these induced velocity integrals be obtained analytically. The alternative is to perform numerical integrations during each production computer run and thus greatly increase the computation time. On the contrary, with the integrations performed analytically, the computing time for the higher-order program is about the same as that of the base method for the same number of panels. (The former is, of course, considerably more accurate.) Not only have general expressions for the integrals been derived, but also simplified expressions to be used to save computing time when the control point in question is far from the panel (refs. 1 and 2). The induced-velocity formulas are presented in section 6.0.

Once the above formulas have been obtained, the potential or velocity induced by the source distribution on a panel at an arbitrary point in space (including any control point) can be written as the sum of six terms, each of which consists of the product of one of the above integral expressions and a certain coefficient. The base-method integral has as its coefficient the unknown value of source density at the control point of the panel itself. For three other integrals, each coefficient consists of the product of this source density and one of the three local curvatures of the surface. The curvatures are evaluated numerically by special procedures, which are outlined in section 7.1. The curvatures are calculated once and for all for each panel before any induced-velocity computation begins. Thus, the above four integrals may be added to obtain a single term whose coefficient is the unknown value of source density at the control point of the panel — an altered "influence coefficient" whose role is exactly analogous to the corresponding coefficient in the base method.

The coefficients of the other two integrals are the unknown derivatives of the source density with respect to distance in two orthogonal directions tangent to the panel. These derivatives must be expressed in terms of the unknown value of source density at the control point of the panel and the values of source density at the control points of the surrounding panels. Once this has been done, the contribution associated with each surrounding value of source density is added to its above-described altered "influence coefficient" to obtain a final "influence coefficient" that expresses the total effect of that value of source density. This is all very simple if the "matrix of influence coefficients" is computed by rows or if it can be stored in the high-speed random-access core of the computer. However, in three-dimensional cases this matrix is computed by columns, and it is normally an order of magnitude too large to fit in core, so large amounts of low-speed storage are required. It is clear from Figure 1 that the panels surrounding a particular panel consist not only of panels on the same strip but also panels on adjacent strips. In the overall numbering scheme of the panels, these latter may be several tens of panels removed from the panel in question.

Accordingly, the task of associating the proper additional influences with these panels is nontrivial. A rather complicated logical scheme involving the use of several auxiliary tape units has been worked out and implemented. This procedure is described in section 8.2.

Similarly the induced velocity due to the vorticity distribution on a panel is a sum of terms, each of which is the product of a first or second derivative of the equivalent dipole distribution (value and first derivatives of vorticity) and some integral expression. Some terms also contain the local geometric curvatures. The above elaborate procedure that accounts for the source derivative effects is required because the source is the basic singularity. Since the vorticity is an auxiliary singularity, simpler procedures may be used to account for its derivatives. The one adopted in the initial version of the present method, which is described in section 9.0, is the simplest of all. It could be made more elaborate and presumably more accurate without greatly complicating the procedure.

5.0 CONSISTENT EXPANSIONS FOR THE POTENTIAL AND VELOCITY INDUCED BY A CURVED PANEL AT A POINT IN SPACE

5.1 The Potential of a Source Distribution

A "true" panel on a body surface is the curved four-sided region of the surface whose corners are input points lying exactly on the surface (figure 3). The boundary curves of the true panel that connect the corner points will be defined shortly. Consider a plane tangent to the surface at some central point of the true panel as yet unspecified. A panel coordinate system is constructed whose origin is the tangency point and whose z or ζ axis is normal to the tangent plane. The x or ξ and y or η axes lie in this plane, and their precise orientation is unimportant for purposes of this section. The corner points of the true panel are projected into the tangent plane along the normal direction. By joining adjacent projected corner points with straight lines, a flat panel is produced, which is assumed to be the projection of the true panel in the tangent plane. This construction now defines the boundary curves of the true panel. They are the curves joining the true corner points that have straight-line projections in the tangent plane.

It is a fundamental assumption of the present method that the dimensions of the panel are small in certain senses. Certainly variations over the panel of the normal direction are assumed small. Moreover, if a physical quantity is expanded in a Maclaurin series, successive terms become small, i.e., if

$$f(\xi,\eta) = \sum_{n=0}^{\infty} \frac{1}{n!} \left(\xi \frac{\partial}{\partial \xi} + \eta \frac{\partial}{\partial \eta}\right)^n_{0,0} f(\xi,\eta) \equiv \sum_{n=0}^{\infty} Q_n(\xi,\eta) \tag{1}$$

then

$$|Q_n| << |Q_m| \qquad \text{if} \qquad m < n \tag{2}$$

Also, the vertical distance ζ of a point on the true panel is of the order of the square of the horizontal distance, i.e.,

$$\zeta = O(\xi^2 + \eta^2) << \sqrt{\xi^2 + \eta^2} \tag{3}$$

The potential at a point (x,y,z) in space due to a source distribution on the true panel is

$$\phi = \iint_S \frac{\sigma}{r}\, dS \tag{4}$$

where

$$r^2 = (x-\xi)^2 + (y-\eta)^2 + (z-\zeta)^2 \tag{5}$$

and where S is the surface area of the true panel. It is desired to express ϕ in terms of a series of integrals over the projected flat panel. Thus it may be stated that the potential of the true panel is "expanded about" that of the flat panel. To illustrate the process more completely, a three-term expansion is derived, although only the first two terms are ultimately retained in the present method.

In panel coordinates the equation $\zeta = f(\xi,\eta)$ of the surface of the true panel may be expanded in a Maclaurin series in the form

$$\zeta = [P\xi^2 + 2Q\xi\eta + R\eta^2] + [T_{30}\xi^3 + T_{21}\xi^2\eta + T_{12}\xi\eta^2 + T_{03}\eta^3] + \ldots \tag{6}$$

$$= \zeta_2 + \zeta_3 + \ldots$$

There are no constant or linear terms in (6) because the origin is at the tangency point. All coefficients in (6) are constants proportional to derivatives of ζ at the origin. The coefficients P, Q, and R, which are the only ones actually used in the present method, are the second derivatives. They are referred to below as the surface curvatures to which they are closely related. The quantity ζ_2 is second order in ξ and η and thus in panel dimension t, and ζ_3 is third order.

The equation of the true panel may be written

$$F(\xi,\eta,\zeta) = \zeta - \zeta_2(\xi,\eta) - \zeta_3(\zeta,\eta) - \ldots = 0 \tag{7}$$

Then, taking the gradient gives

$$\text{grad } F = \vec{k} - (\zeta_{2\xi} + \zeta_{3\xi} + \ldots)\vec{i} - (\zeta_{2\eta} + \zeta_{3\eta} + \ldots)\vec{j} \tag{8}$$

where subscripts ξ and η denote partial derivatives and $\vec{i}$, $\vec{j}$, $\vec{k}$ are the unit vectors of the panel coordinate system. The vector grad F is normal

to the panel at any point. The unit normal at any point is

$$\vec{n} = \frac{\text{grad } F}{|\text{grad } F|} \tag{9}$$

so the ζ-component of the unit normal is

$$n_\zeta = \frac{1}{|\text{grad } F|} = \frac{1}{\sqrt{1 + (\zeta_{2\xi} + \zeta_{3\xi} + \ldots)^2 + (\zeta_{2\eta} + \zeta_{3\eta} + \ldots)^2}} \tag{10}$$

This can be expanded in the form

$$n_\zeta = 1 - \frac{1}{2}\left[(\zeta_{2\xi} + \zeta_{3\xi} + \ldots)^2 + (\zeta_{2\eta} + \zeta_{3\eta} + \ldots)^2\right]$$

$$+ \frac{3}{8}\left[(\zeta_{2\xi} + \zeta_{3\xi} + \ldots) + (\zeta_{2\eta} + \zeta_{3\eta} + \ldots)^2\right]^2 + \ldots \tag{11}$$

From (6) it is clear that $\zeta_{2\xi}$ and $\zeta_{2\eta}$ are first order, $\zeta_{3\xi}$ and $\zeta_{3\eta}$ are second order, etc., so the leading terms from the first square bracket of (11) are second order, and the leading terms in the second square bracket are fourth order. Thus,

$$n_\zeta = 1 - \frac{1}{2}(\zeta_{2\xi}^2 + \zeta_{2\eta}^2) \tag{12}$$

is a valid three-term expansion with second (linear) term zero. More precisely,

$$\begin{aligned} n_\zeta &= 1 - \frac{1}{2}\left[(2P\xi + 2Q\eta)^2 + (2Q\xi + 2R\eta)^2\right] \\ &= 1 - 2\left[(P^2 + Q^2)\xi^2 + 2(PQ + QR)\xi\eta + (Q^2 + R^2)\eta^2\right] \\ n_\zeta &= 1 - 2\psi_2 \end{aligned} \tag{13}$$

where ψ_2 is second order. The elementary surface area dS on the true panel is related to the elementary area $dA = d\xi d\eta$ in the tangent plane by

$$n_\zeta dS = dA \tag{14}$$

$$dS = (1 + 2\psi_2)d\xi d\eta \tag{15}$$

The source density is strictly a function of surface distances along the panel. However, it can be shown that there is no difference between surface distances

and ξ and η through second order. Thus it suffices to define σ in terms of ξ and η in the form

$$\sigma = \sigma_o + (\sigma_x \xi + \sigma_y \eta) + (\sigma_{xx} \xi^2 + 2\sigma_{xy} \xi\eta + \sigma_{yy} \eta^2) + \ldots$$

$$= \sigma_o + \sigma_1 + \sigma_2 \tag{16}$$

where σ_n is n-th order in ξ and η and thus in panel dimension t. The coefficients in (16) are constants proportional to derivatives of σ at the origin.

Thus, to three terms

$$\begin{aligned} \sigma dS &= (\sigma_o + \sigma_1 + \sigma_2)(1 + 2\psi_2) d\xi d\eta \\ &= (\sigma_o + \sigma_1 + \sigma_2') d\xi d\eta \end{aligned} \tag{17}$$

where

$$\sigma_2' = \sigma_2 + 2\psi_2 \tag{18}$$

All of the above expansions are independent of the location of the point (x,y,z).

It remains to expand 1/r, which of course, does depend on x,y,z. It is necessary to differentiate three ranges of value of r:

(a)	$r \gg t$	for all ξ,η	
(b)	$r = O(t)$	for all ξ,η	(19)
(c)	$r \ll t$	for some ξ,η	
	$r = O(t)$	for other ξ,η	

In words, the ranges amount to the situations where the distance of the point (x,y,z) from the origin of panel coordinates is, respectively large, of the order of, and small compared to the dimensions of the panel. It turns out that the range (b) where r is of the order of the panel dimensions is the essential one. In the far-field, range (a), 1/r is expanded in negative powers of $r_o = (x^2 + y^2 + z^2)^{\frac{1}{2}}$. The resulting expansion differs in no important way from the usual far-field multipole expansion and thus is relatively easy to derive. An order-of-magnitude comparison of the expansions of ranges (a) and (b) shows that while certain terms become small faster than others as the distance r increases, the expansion derived for range (b)

is valid for range (a), although it is conservative in that some retained terms could be eliminated. For points close to the panel, range (c), it is necessary to assume that they lie on a line through the origin having a finite slope with respect to the tangent plane. Under this condition the order-of-magnitude analysis of range (b) remains valid. This is just what the physics of a panel method requires in any event. Eventually, the control point of the panel is identified with the origin of panel coordinates and the above condition states that if a point approaches the surface, it does so at a control point. Since it is only at the control points that the normal velocity boundary condition is applied, approaching any other surface point would give physically meaningless results. Thus the derivation below concentrates on range (b), which may be thought of as the effect of a panel on control points of nearby panels.

The distance r can be written

$$r^2 = (x-\xi)^2 + (y-\eta)^2 + z^2 - 2z\zeta + \zeta^2$$
$$= r_f^2 - 2z\zeta + \zeta^2 \tag{20}$$

where r_f is the distance between (x,y,z) and the point $(\xi,\eta,0)$ on the flat panel (Figure 3). Thus

$$\frac{1}{r} = \frac{1}{r_f}\,\frac{1}{\sqrt{1 + (-2z\zeta + \zeta^2)/r_f^2}} = \frac{1}{r_f}\left[1 - \frac{1}{2}\,\frac{-2z\zeta + \zeta^2}{r_f^2} + \frac{3}{8}\,\frac{4z^2\zeta^2}{r_f^4} + \cdots\right]$$
$$= \frac{1}{r_f}\left[1 + \frac{z}{r_f}\,\frac{\zeta}{r_f} + \left(\frac{3}{2}\,\frac{z^2}{r_f^2} - \frac{1}{2}\right)\frac{\zeta^2}{r_f^2} + \cdots\right] \tag{21}$$

Note that (z/r_f) is of order unity, and, since r_f is $O(t)$, the quantity ζ/r_f is also $O(t)$, i.e., $O(\xi)$. If use is made of (6), the above becomes

$$\frac{1}{r} = \frac{1}{r_f}\left[1 + \frac{z}{r_f}\,\frac{\zeta_2 + \zeta_3 + \cdots}{r_f} + \left(\frac{3}{2}\,\frac{z^2}{r_f^2} - \frac{1}{2}\right)\left(\frac{\zeta_2 + \zeta_3 + \cdots}{r_f}\right)^2\right]$$

from which the desired three-term expansion is obtained in the form

$$\frac{1}{r} = \frac{1}{r_f}\left\{1 + \frac{z}{r_f}\,\frac{\zeta_2}{r_f} + \left[\frac{z}{r_f}\,\frac{\zeta_3}{r_f} + \left(\frac{3}{2}\,\frac{z^2}{r_f^2} - \frac{1}{2}\right)\frac{\zeta_2^2}{r_f^2}\right]\right\} \tag{22}$$

or, for abbreviation,

$$\frac{1}{r} = \frac{1}{r_f}(1 + c_1 + c_2) \tag{23}$$

where c_n is of order n in ξ or η and thus in t. Now this is multiplied by (17) to obtain the expansion

$$\begin{aligned}\frac{\sigma}{r}\,dS &= \frac{1}{r_f}(\sigma_o + \sigma_1 + \sigma_2')(1 + c_1 + c_2)dA \\ &= \frac{dA}{r_f}[\sigma_o + \sigma_1 + \sigma_2' \\ &\quad + c_1\sigma_o + c_1\sigma_1 + c_1\sigma_2' \\ &\quad + c_2\sigma_o + c_2\sigma_1 + c_2\sigma_2']\end{aligned} \tag{24}$$

The square bracket in (24) must be reduced to a three-term expansion using the facts that

$$\sigma_o >> \sigma_1 >> \sigma_2 \tag{25}$$

and

$$1 >> c_1 >> c_2 \tag{26}$$

The leading (lowest order) term is clearly σ_o because all terms are small compared to it. Possible members of the second term are σ_1 and $c_1\sigma_o$ because all remaining terms are small compared to one or the other. Thus, both of these are retained in the second term, because neither can be guaranteed to be small compared to the other in all cases. The question then arises as to which of the remaining six terms of the square bracket of (24) need to be retained in the third term of the expansion. Obviously, if any of these six is small compared to any other, it may be discarded. This eliminates all but σ_2, $c_1\sigma_1$, and $c_2\sigma_o$. Thus, the three-term expansion of the integrand of (4) has the form

$$\frac{\sigma}{r}\,dS = \frac{dA}{r_f}[\sigma_o + (c_1\sigma_o + \sigma_1) + (c_2\sigma_o + c_1\sigma_1 + \sigma_2')] \tag{27}$$

when the abbreviations of (16) and (24) are replaced by their actual expressions, the three-term expansion of (4) is

$$\phi = \sigma_o \iint_A \frac{dA}{r_f} + \left[\sigma_o \iint_A z \frac{\zeta_2}{r_f^3} \, dA + \iint_A \frac{\sigma_x \xi + \sigma_y \eta}{r_f} \, dA \right]$$

$$+ \left[\sigma_o \iint_A \left(z \frac{\zeta_3}{r_f^3} + \frac{3}{2} z^2 \frac{\zeta_2^2}{r_f^5} - \frac{1}{2} \frac{\zeta_2^2}{r_f^3} \right) + \iint_A z \frac{\zeta_2}{r_f^3} (\sigma_x \xi + \sigma_y \eta) dA \right] \qquad (28)$$

$$+ \iint_A \frac{1}{r_f} \left[\sigma_{xx} \xi^2 + 2\sigma_{xy} \xi\eta + \sigma_{yy} \eta^2 + 2(P^2 + Q^2)\xi^2 + 4(PQ + QR)\xi\eta \right.$$

$$\left. + 2(Q^2 + R^2)\eta^2 \right] dA$$

where the integrals are over the projected flat panel. Defining the integrals,

$$I_{mnp} = \iint_A \frac{\xi^m \eta^n}{r_f^p} \, dA \qquad (29)$$

the three-term expansion of the potential can be written

$$\phi = \phi^{(o)}\sigma_o + \left[\phi^{(c)}\sigma_o + \phi^{(1x)}\sigma_x + \phi^{(1y)}\sigma_y \right] \qquad (30)$$

$$+ \left[\phi^{(20)}\sigma_o + \phi^{(2x)}\sigma_x + \phi^{(2y)}\sigma_y + \phi^{(2xx)}\sigma'_{xx} + 2\phi^{(2xy)}\sigma'_{xy} + \phi^{(2yy)}\sigma'_{yy} \right]$$

where

$$\sigma'_{xx} = \sigma_{xx} + 2(P^2 + Q^2)$$

$$\sigma'_{xy} = \sigma_{xy} + 2(PQ + QR) \qquad (31)$$

$$\sigma'_{yy} = \sigma_{yy} + 2(Q^2 + R^2)$$

The individual potentials in (30) are

$$\phi^{(o)} = I_{001} \qquad (32)$$

$$\phi^{(c)} = z[PI_{203} + 2QI_{113} + RI_{023}] \qquad (33)$$

$$\phi^{(1x)} = I_{101}$$

$$\phi^{(1y)} = I_{011} \qquad (34)$$

$$\phi^{(20)} = z[T_{30}I_{303} + T_{21}I_{213} + T_{12}I_{123} + T_{03}I_{033}]$$
$$+ \frac{3}{2} z^2 [P_2 I_{405} + 4PQI_{315} + (2PR + 4Q^2)I_{225} + 4QRI_{135} + R^2 I_{045}]$$
$$- \frac{1}{2} [P^2 I_{403} + 4PQI_{313} + (2PR + 4Q^2)I_{223} + 4QRI_{133} + R^2 I_{043}] \qquad (35)$$

$$\phi^{(2x)} = z[PI_{303} + 2QI_{213} + RI_{123}]$$
$$\phi^{(2y)} = z[PI_{213} + 2QI_{123} + RI_{033}] \qquad (36)$$

$$\phi^{(2xx)} = I_{201}$$
$$\phi^{(2xy)} = I_{111} \qquad (37)$$
$$\phi^{(2yy)} = I_{021}$$

The first term of (30), $\phi^{(o)}\sigma_o$, corresponds to a flat panel with a constant source density. This is, of course, the term used in the base method. The second term of (30) contains the second derivatives P, Q, and R, but no higher derivatives, of the surface shape and contains the first derivatives of the source density, but no higher derivatives. Thus the second term of (30) corresponds to a paraboloidal panel shape with a linearly varying source density. The third term of (30) contains all the preceeding quantities and also the third derivatives of the surface shape and the second derivatives of the source density: a cubic panel with a quadratic source density.

The equations above illustrate the fact that succeeding terms in the expansion for the potential of a panel increase rapidly in complexity. A single first term is followed by a second term containing five individual parts, each with its own integral of the form (29). The third term contains 23 individual parts which together involve 17 different integrals of the form (29). The great increase in complexity associated with retaining the third term of (30) appears to be unjustified at this time. Accordingly, the higher-order method accounts for the source density effect by considering the first two terms of (30). This is the approach that has previously been followed in the two-dimensional and axisymmetric higher-order methods, references 5 and 6.

5.2 The Potential of a Dipole Distribution

This parallels almost exactly the development of section 5.1 for the effect of a source distribution on a panel, as sketched in figure 3. If the dipole strength is $\mu(\xi,\eta)$ the potential of the true panel is

$$\phi_d = \iint_S \left[\vec{n} \cdot \text{grad}_{\xi\eta\zeta} \left(\frac{1}{r}\right)\right] \mu dS = \iint_S d\phi_d \tag{38}$$

where as before $\vec{n}$ is the unit normal vector to the true panel. From equations (7) through (13) it is known that (13) is a valid three term expansion of both the ζ-component of $\vec{n}$ and of $|\text{grad } F|^{-1}$. Expansions of the other two components of the normal vector are

$$\begin{aligned} n_\xi &= -(\zeta_{2\xi} + \zeta_{3\xi})n_\zeta \\ n_\eta &= -(\zeta_{2\eta} + \zeta_{3\eta})n_\zeta \end{aligned} \tag{39}$$

Only two terms are required because these two are respectively of first and second order in ξ and η while n_ζ has a zero order term. Thus

$$\vec{n} \cdot \text{grad}\left(\frac{1}{r}\right) = \frac{n_\zeta}{r^3} [-(\zeta_{2\xi} + \zeta_{3\xi})(x - \xi) - (\zeta_{2\eta} + \zeta_{3\eta})(y - \eta) + z - \zeta] \tag{40}$$

is a valid three-term expansion, and it is clear retention of third terms in (39) would produce fourth terms in (40). When use is made of (14) the integrand of (38) becomes

$$\begin{aligned} d\phi_d = \{z - [\zeta_2 + \zeta_{2\xi}(x - \xi) + \zeta_{2\eta}(y - \eta)] \\ - [\zeta_3 + \zeta_{3\xi}(x - \xi) + \zeta_{3\eta}(y - \eta)]\} \frac{\mu_0 + \mu_1 + \mu_2}{r^3} dA \end{aligned} \tag{41}$$

where

$$\begin{aligned} \mu_0 &= \text{const} \\ \mu_1 &= \mu_x \xi + \mu_y \eta \\ \mu_2 &= \mu_{xx}\xi^2 + 2\mu_{xy}\xi\eta + \mu_{yy}\eta^2 \end{aligned} \tag{42}$$

and where the terms in the curly bracket have been arranged in increasing order.

From (23)

$$\frac{1}{r^3} = \frac{1}{r_f^3}(1 + c_1 + c_2)^3$$
$$= \frac{1}{r_f^3}[1 + 3c_1 + 3(c_1^2 + c_2)] \tag{43}$$

By reasoning similar to that following equation (26) a valid three-term expansion is

$$\frac{\mu}{r^3} = \frac{1}{r_f^3}\{\mu_o + [3c_1\mu_o + \mu_1] + [3(c_1^2 + c_2)\mu_o + 3c_1\mu_1 + \mu_2]\} \tag{44}$$

Finally a valid three-term expansion of (41) is

$$d\phi_d = \frac{1}{r_f^3}\Big\{z\mu_o + \{z(3c_1\mu_o + \mu_1) - [\zeta_2 + \zeta_{2\xi}(x-\xi) + \zeta_{2\eta}(y-\eta)]\mu_o\}$$
$$+ \{z[3(c_1^2 + c_2)\mu_o + 3c_1\mu_1 + \mu_2] - [\zeta_2 + \zeta_{2\xi}(x-\xi) + \zeta_{2\eta}(y-\eta)](3c_1\mu_o + \mu_1)$$
$$- [\zeta_3 + \zeta_{3\xi}(x-\xi) + \zeta_{3\eta}(y-\eta)]\mu_o\}\Big\}dA \tag{45}$$

The problem with using dipoles is that the three-term expansion (45) of the dipole potential (38) is equivalent in accuracy to a two-term expansion of the source potential (4) obtained by truncating (30). This can be verified in several ways. Mathematically it is straightforward to verify that when x,y,z and r_f are of order ξ and η and thus of the order of element dimension t, each term of (45) is one order lower than the corresponding term of (30). For example the leading terms are

$$\sigma_o/r_f = \sigma_o O(t^{-1})$$
$$z\mu_o/r_f^3 = \mu_o O(t^{-2}) \tag{46}$$

Some physical insight can be obtained by performing the integration for the first term of (45) which corresponds to a constant-strength dipole distribution. The result is the potential of a concentrated vortex filament lying around the edges of the panel. Clearly no such singularity can exist on the body surface. It is present only because an isolated panel has been considered, and it must cancel (at least to some order) with similar singularities on the surrounding panels. Thus, when only noncancelling terms are considered, a valid two-term expansion of (38) consists of the second and third terms of (45), which, as mentioned above, correspond in their orders

to the first two terms of (30). Unfortunately they are much more complicated. Integration of the third term of (45) leads to an expression even more complicated than the third term of (30). Another difficulty is that the third derivatives of the surface shape enter into the third term of (45) through ζ_3 and its derivatives. Thus, although only quadratic dipole terms, which correspond to linear vorticity terms, are included in (45), it would appear that a cubic panel is required. However, this turns out to be only apparently true.

Most of the difficulty with the expansion (45) arises from the fact that it expresses the effect not only of a distributed vorticity distribution over the panel, but also of a concentrated vortex filament around the panel edges. As mentioned above, the first term represents a constant-strength vortex filament and no distributed vorticity at all. The second and third terms contain mixtures of effects due to distributed vorticity and those due to variable-strength vortex filaments around the panel edges. In particular, all the third derivative terms enter only by way of these "edge vortex" terms. Clearly all edge vortex terms must cancel with those of adjacent panels. The result must be a much-simplified expansion and one that does not contain any third derivative terms. Unfortunately, it does not appear possible to accomplish this cancellation analytically. Certainly it is necessary to use the integrated form of (45), because the cancellation is not an identity in the integrand, but only in the final result. Even if this is done, the effects of the distributed vorticity and those of the edge vortex are not neatly separated but are combined into some of the analytic expressions. Clearly all terms containing μ_0 should cancel, but it is not sufficient simply to drop these from (45). Unless all cancelling terms can be identified and eliminated, the deletion of some of them leads to a disruption of the cancellation process.

5.3 The Velocity Due to a Vorticity Distribution

The situation described in section 5.2 is present also in two dimensions. Indeed, the considerations of the previous section regarding cancellation, etc., can be illustrated most easily with two-dimensional examples. Difficulties are avoided in two dimensions by considering a vorticity distribution on the panel rather than a dipole distribution. In such a case all the

consistency arguments of section 5.1 can be invoked, because the velocity due to vorticity is simply that due to the same distribution of source strength rotated through a right angle. This approach simply ignores edge vortex terms on the presumption that they cancel with those of adjacent panels.

The present method applies this technique to the three-dimensional case, i.e., it uses a linearly-varying vorticity distribution over the panel and ignores edge vortex effects. (Reference 1 gives specific proof of the relation between dipole and vorticity distributions and the edge vortex.) There are, of course, some differences between the two-dimensional and the three-dimensional cases. The most obvious theoretical danger arises from the fact that the velocity field due to a vorticity distribution is in general nonpotential with edge vorticies neglected. To the extent that edge vortex cancellation with adjacent panels is less than exact, the final velocity field about the body is nonpotential. However, this does not appear to be serious. Any panel method is an approximation to the exact potential flow with calculational errors of some higher order that approach zero with increasing panel number. There is no obvious reason why a method whose calculation error is potential should be preferred to one whose error is not. There are, however, two features of the use of vorticity worth mentioning. Surface vorticity is an auxiliary singularity in the sense of section 3.0. While its variation over a single panel is linear, its global variation over the body as a whole is legislated by what may be termed "assembly formulas" (section 9.0) that contain just enough free parameters to permit satisfaction of the Kutta condition on the trailing-edge segments (figure 1). It is important that the assembly formulas insure approximate continuity of the dipole strength that is equivalent to the surface vorticity so that edge vortex effects, in fact, approximately cancel. In particular, the step-function spanwise variation of bound vorticity (ref. 1), which is ordinarily used with the base method, is not appropriate for use with the higher-order surface vorticity. Finally it is clear that at any actual edges of the body where a concentrated vortex filament is truly required, special edge-vortex formulas must be incorporated into the method. The most common such situation is a wing tip with a nonzero chord, if the equivalent dipole strength is not forced to go to zero there. In practical cases only a small percentage of the panels would require these additional formulas. However, at this time edge-vortex formulas have not been included, so that the method

is not applicable to any body requiring edge vortices. Inclusion of edge-vortex formulas is seemingly a desirable modification of the method. In the meantime, however, cases requiring edge vortices must be avoided. For example, a wing-tip is handled either by closing the tip to a point or by having the assembly formulas force the equivalent dipole strength to zero at the tip. This last can be accomplished in a routine manner using the piecewise-linear spanwise vorticity variation (section 9.4). Either or both of these procedures should give satisfactory results for a normal wing tip. However, a partial-span deflected flap may be more difficult and requires further study.

The effect of a vorticity distribution on a panel cannot be expressed in terms of a potential, as mentioned above. The velocity induced by the panel of figure 3 at a point (x,y,z) is

$$\vec{v}_w = \iint_S \frac{\vec{\omega} \times \vec{r}}{r^3} \, dS \tag{47}$$

where $\vec{\omega}$ is the vector vorticity strength and

$$\vec{r} = (x - \xi)\vec{i} + (y - \eta)\vec{j} + (z - \zeta)\vec{k} \tag{48}$$

The distance r has its usual meaning (5), which is also equal to $|\vec{r}|$, and the integral is over the true panel. To insure that the vorticity satisfies the usual vorticity conservation theorems over the panel, it is convenient to express $\vec{\omega}$ in terms of an equivalent dipole distribution μ. As shown in reference 1, the relation is

$$\vec{\omega} = -\vec{n} \times \text{grad } \mu \tag{49}$$

where $\vec{n}$ is the unit normal vector (9), whose components η_ξ, η_η, η_ζ are given by (13) and (39). To be compatible with the source density and panel-geometry expansions, μ is taken to be a quadratic function of panel coordinates ξ and η in

$$\mu = \mu_o + \mu_x \xi + \mu_y \eta + \mu_{xx} \xi^2 + \mu_{xy} \xi\eta + \mu_{yy} \eta^2 \tag{50}$$

so that the components of $\vec{\omega}$ vary linearly over the panel. Furthermore, since a two-term expansion of the source potential (4) is all that appears feasible, only a two-term expansion of (47) is required. Evidently

$$\frac{\partial \mu}{\partial \xi} = \mu_x + 2(\mu_{xx}\xi + \mu_{xy}\eta) \tag{51}$$

$$\frac{\partial \mu}{\partial \eta} = \mu_y + 2(\mu_{xy}\xi + \mu_{yy}\eta)$$

are two-term expansions of the components of gradμ. Then (49) gives

$$\vec{\omega} = (n_\zeta \frac{\partial \mu}{\partial \eta})\vec{i} - (n_\zeta \frac{\partial \mu}{\partial \xi})\vec{j} + (n_\eta \frac{\partial \mu}{\partial \xi} - n_\xi \frac{\partial \mu}{\partial \eta})\vec{k} \tag{52}$$

Two-term expansions of the $\vec{i}$ and $\vec{j}$ components of (52) contain zeroth and first-order terms. Since the leading term of the $\vec{k}$ component is linear only that one term is required. The two-term expansion of (52) is

$$\begin{aligned}\vec{\omega} &= [\mu_y + 2(\mu_{xy}\xi + \mu_{yy}\eta)]\vec{i} - [\mu_x + 2(\mu_{xx}\xi^2 + \mu_{xy}\eta^2)]\vec{j} + [-\zeta_{2\eta}\mu_x + \zeta_{2\xi}\mu_y]\vec{k} \\ &= \omega_\xi \vec{i} + \omega_\eta \vec{j} + \omega_\zeta \vec{k}\end{aligned} \tag{53}$$

Also needed is

$$\begin{aligned}\vec{\omega} \times \vec{r} = \quad & [\omega_\eta(z - \zeta) - \omega_\zeta(y - \eta)]\vec{i} \\ & + [\omega_\zeta(x - \xi) - \omega_\xi(z - \zeta)]\vec{j} \\ & + [\omega_\xi(y - \eta) - \omega_\eta(x - \xi)]\vec{k}\end{aligned} \tag{54}$$

For the present purpose the expansion (43) for r^{-3} may be truncated after two terms, i.e.,

$$\frac{1}{r^3} = \frac{1}{r_f^3}(1 + 3c_1) = \frac{1}{r_f^3}\left(1 + 3\frac{z\zeta_2}{r_f^2}\right) \tag{55}$$

Moreover to the order being considered $n_\xi = 1$, and thus $dS = dA$ (15). If now the components of (47) are written

$$V_{\omega x} = \iint_A dV_{\omega x}, \qquad V_{\omega y} = \iint_A dV_{\omega y}, \qquad V_{\omega z} = \iint_A dV_{\omega z} \tag{56}$$

the integrands are

$$dV_{\omega x} = \left\{-\frac{z}{r_f^3}\mu_x + \frac{J_x}{r_f^3} - 3z^2\mu_x\frac{\zeta_2}{r_f^5}\right\}dA$$

$$dV_{\omega y} = \left\{ -\frac{z}{r_f^3}\mu_y + \frac{J_y}{r_f^3} - 3z^2\mu_y \frac{\zeta_2}{r_f^5} \right\} dA \tag{57}$$

$$dV_{\omega z} = \left\{ \frac{I_z}{r_f^3} + \frac{J_z}{r_f^3} + 3zI_z \frac{\zeta_2}{r_f^5} \right\} dA$$

where

$$I_z = (x-\xi)\mu_x + (y-\eta)\mu_y$$

$$J_x = -2z(\mu_{xx}\xi + \mu_{xy}\eta) + \mu_x\zeta_2 + (\zeta_{2\eta}\mu_x - \zeta_{2\xi}\mu_y)(y-\eta) \tag{58}$$

$$J_y = -2z(\mu_{xy}\xi + \mu_{yy}\eta) + \mu_y\zeta_2 + (-\zeta_{2\eta}\mu_x + \zeta_{2\xi}\mu_y)(x-\xi)$$

$$J_z = 2[(\mu_{xx}\xi + \mu_{xy}\eta)(x-\xi) + (\mu_{xy}\xi + \mu_{yy}\eta)(y-\eta)]$$

In each of the three components of (57), the first term is the leading one with a magnitude $O(t^{-2})$ neglecting the factor dA. These leading terms correspond to a constant vorticity on a flat panel. The second and third terms in each component of (57) have the same magnitude $O(t^{-1})$ and together comprise the higher-order term of the expansion. The third term is a pure curvature effect, while the second term has both curvature and vorticity derivative effects.

Regardless of their physical nature, the second terms of (57) have the mathematical form of potentials of linear and quadratic dipoles on a flat panel, and thus they can be evaluated by the formulas of reference 1. The same is true of the first terms. Only the third terms of (57) require new analytic formulas.

The above considerations make it convenient to consider the vortex velocity as a sum of the three terms in the form

$$V_{\omega x} = V_{\omega x}^{(0)} + V_{\omega x}^{(1)} + V_{\omega x}^{(2)}$$

$$V_{\omega y} = V_{\omega y}^{(0)} + V_{\omega y}^{(1)} + V_{\omega y}^{(2)} \tag{59}$$

$$V_{\omega z} = V_{\omega z}^{(0)} + V_{\omega z}^{(1)} + V_{\omega z}^{(2)}$$

where the superscripts 0, 1, 2 denote, respectively, integrals of the first, second, and third terms of (57).

6.0 INTEGRATED INDUCED VELOCITY FORMULAS FOR A PANEL

6.1 General Remarks

This section presents detailed formulas for the velocity induced by an individual panel at a point in space. These formulas are obtained from the expressions developed in section 5.0 by performing the indicated integrations over the flat projected panel. Different procedures are called for depending on the distance of the point in question from the panel. For nearby points the expressions of section 5.0 are integrated exactly. This procedure is rather lengthy and details are omitted. Only the final formulas for this "Near Field" are presented, and these are the key to the present method. As in reference 1, it is assumed that the point in question has been transformed into the panel coordinate system and all Near-Field formulas are given in terms of this coordinate system. For points further from the panel, the integrals of section 5.0 are evaluated by a classic multipole expansion (refs. 1 and 2). The orders of the expansions are selected to be at least as high as the terms in question. This is a relatively simple procedure analytically, and the resulting "Intermediate Field" formulas require much less computing time than the Near-Field formulas. This computation also is carried out in panel coordinates. For points even further away, a "Far-Field" approximation is used. This is obtained simply by retaining only the first terms in the multipole expansions. However, for the source effects and some of the vorticity effects, the Far-Field formulas have been put in vector form, and thus they can be evaluated directly in the so-called reference coordinate system in which the body is input. This eliminates the need for transformations and further reduces computing time. Certain terms in the vorticity effects have such complicated Far-Field expressions that it did not seem worthwhile to put them in vector form. Accordingly, they are evaluated in panel coordinates as is done in the Near- and Intermediate-Fields. Thus, in section 6.0 all individual coordinates and vector components are in panel coordinates. Expressions in vector form may be evaluated in the reference coordinate system.

The entire philosophy of the induced velocity computation and all of the associated bookkeeping details are identical to those of reference 1, to which

the reader is referred. The procedure for the multipole expansion has already been mentioned. Other matters are the ranges of distance adopted for Near-, Intermediate- and Far-Fields, transformations between panel and reference coordinate systems, and geometric quantities defining the projected flat panels. In addition, many of the induced-velocity expressions developed in reference 1 enter the formulas of the present method. To report these would add greatly to the length of the present report, so again reference 1 is relied on. The panel is assumed to have two parallel sides, as illustrated in figure 20 of reference 1.

6.2 Source Velocity Formulas

The source potential is given in equations (30) and (33) of section 5.1. The velocity induced by the panel is obtained by taking the negative gradient to obtain

$$\vec{V} = \vec{V}^{(0)}_{\sigma_o} + [P\vec{V}^{(P)} + 2Q\vec{V}^{(Q)} + R\vec{V}^{(R)}] + \vec{V}^{(1x)}_{\sigma_x} + \vec{V}^{(1y)}_{\sigma_y} \qquad (60)$$

where each individual velocity is the negative gradient of the corresponding potential.

6.2.1 Near Field

The velocity components are:

$$\left.\begin{aligned} V_x^{(0)} &= V_x \text{ (source)} \\ V_y^{(0)} &= V_y \text{ (source)} \\ V_z^{(0)} &= V_z \text{ (source)} \end{aligned}\right\} \quad \text{eq. (7.7.7), reference 1} \qquad (61)$$

$$\left.\begin{aligned} V_x^{(R)} &= -\frac{\partial \phi_{02}}{\partial x}, \quad & V_x^{(Q)} &= -\frac{\partial \phi_{11}}{\partial x} \\ V_y^{(R)} &= -\frac{\partial \phi_{02}}{\partial y}, \quad & V_y^{(Q)} &= -\frac{\partial \phi_{11}}{\partial y} \\ V_z^{(R)} &= -\frac{\partial \phi_{02}}{\partial z}, \quad & V_z^{(Q)} &= -\frac{\partial \phi_{11}}{\partial z} \end{aligned}\right\} \quad \begin{array}{l}\text{eqs. (7.7.14) and (7.7.17)} \\ \text{reference 1}\end{array} \qquad (62)$$

$$V_x^{(P)} = -\left[z\frac{\partial J_{20}}{\partial x} + 2x\frac{\partial \phi_{10}}{\partial x} - x^2\frac{\partial \phi_{00}}{\partial x} - 2zV_x\ (\text{source})\right]$$

$$V_y^{(P)} = -\left[z\frac{\partial J_{20}}{\partial y} + 2x\frac{\partial \phi_{10}}{\partial y} - x^2\frac{\partial \phi_{00}}{\partial y}\right] \qquad (63)$$

$$V_z^{(P)} = -\left[z\frac{\partial J_{20}}{\partial z} + 2x\frac{\partial \phi_{10}}{\partial z} - x^2\frac{\partial \phi_{00}}{\partial z} + J_{20}\right]$$

where all derivatives except J_{20} are given in equations (7.7.9) through (7.7.11) of reference 1, and where

$$J_{20} = \phi(\text{source}) - H_{02} \qquad (64)$$

$$\frac{\partial J_{20}}{\partial x} = -V_x(\text{source}) - \frac{\partial H_{02}}{\partial x}, \qquad \frac{\partial J_{20}}{\partial y} = -V_y(\text{source}) - \frac{\partial H_{02}}{\partial y}$$

$$\frac{\partial J_{20}}{\partial z} = -V_z(\text{source}) - \frac{\partial H_{02}}{\partial z} \qquad (65)$$

H_{02} and its derivatives are given in equations (7.7.15) and (7.7.16) of reference 1, and

$$\phi(\text{source}) = (y-\eta_1)L^{(12)} + \frac{(x-\xi_2) - m_{32}(y-\eta_2)}{\sqrt{1+m_{32}^2}}\,L^{(23)}$$

$$-(y-\eta_3)L^{(34)} - \frac{(x-\xi_4) - m_{41}(y-\eta_4)}{\sqrt{1+m_{41}^2}}\,L^{(41)} - zV_z(\text{source}) \qquad (66)$$

The undefined quantities in (66) are given in section 7.2 and equation (7.7.3) of reference 1.

$$V_x^{(1x)} = xV_x\ (\text{source}) - J_{20}$$

$$V_y^{(1x)} = xV_y\ (\text{source}) - J_{11} \qquad (67)$$

$$V_z^{(1x)} = xV_z\ (\text{source}) - zV_x\ (\text{source})$$

$$V_x^{(1y)} = yV_x \text{ (source)} - J_{11}$$
$$V_y^{(1y)} = yV_y \text{ (source)} - J_{02} \tag{68}$$
$$V_z^{(1y)} = yV_z \text{ (source)} - zV_y \text{ (source)}$$

$$J_{02} = H_{02} - zV_z \text{ (source)} \tag{69}$$

6.2.2 Intermediate Field

Unlike the near-field, where many of the definitions of reference 1 can be used without change, the intermediate-field formulas must be modified by the inclusion of terms involving first moments of the panel area. These are no longer zero because the panel centroid is no longer used as origin.

Thus, for example, equation (7.6.7) of reference 1 is modified to

$$V_x^{(0)} = \frac{t^2}{r_o^2}\left\{-I_{00}u_x + \left(\frac{t}{r_o}\right)[I_{10}u_{xx} + I_{01}u_{xy}] + \left(\frac{t}{r_o}\right)^2 [I_{20}u_{xxx} + 2I_{11}u_{xxy} + I_{02}u_{xyy}]\right\}$$

$$V_y^{(0)} = \frac{t^2}{r_o^2}\left\{-I_{00}u_y + \left(\frac{t}{r_o}\right)[I_{10}u_{xy} + I_{01}u_{yy}] + \left(\frac{t}{r_o}\right)^2 [I_{20}u_{xxy} + 2I_{11}u_{xyy} + I_{02}u_{yyy}]\right\} \tag{70}$$

$$V_z^{(0)} = \frac{t^2}{r_o^2}\left\{-I_{00}u_z + \left(\frac{t}{r_o}\right)[I_{10}u_{xz} + I_{01}u_{yz}] + \left(\frac{t}{r_o}\right)^2 [I_{20}u_{xxz} + 2I_{11}u_{xyz} + I_{02}u_{yyz}]\right\}$$

$$\left.\begin{aligned} V_x^{(R)} &= -\frac{\partial\phi_{02}}{\partial x}, & V_x^{(Q)} &= -\frac{\partial\phi_{11}}{\partial x} \\ V_y^{(R)} &= -\frac{\partial\phi_{02}}{\partial y}, & V_y^{(Q)} &= -\frac{\partial\phi_{11}}{\partial y} \\ V_z^{(R)} &= -\frac{\partial\phi_{02}}{\partial z}, & V_z^{(Q)} &= -\frac{\partial\phi_{11}}{\partial z} \end{aligned}\right\} \text{ eqs. (7.6.11) and (7.6.12), reference 1} \tag{71}$$

It should be noted that early versions of reference 1 were missing a factor of 1/2 in the 2nd order terms of these equations. It should be further noted that when the derivatives of the flat-panel dipole potentials, ϕ_{00}, ϕ_{01} and

ϕ_{10} are being evaluated in the intermediate field from equations (7.6.8), (7.6.9) and (7.6.10) of reference 1, not only should the second-order terms be multiplied by a 1/2 (if such a factor is not already present), but also all "crossed out" terms should be included. This last is due to the fact that the panel centroid is no longer used as origin of panel coordinates and thus the first moments I_{10} and I_{01} are not zero.

$$V_x^{(P)} = -\frac{\partial \phi_{20}}{\partial x}$$

$$V_y^{(P)} = -\frac{\partial \phi_{20}}{\partial y} \qquad (72)$$

$$V_z^{(P)} = -\frac{\partial \phi_{20}}{\partial z}$$

where ϕ_{20} and its derivatives are given by

$$\phi_{20} = -\frac{t^4}{r_o^2}\left\{I_{20}u_z - \left(\frac{t}{r_o}\right)[I_{30}u_{xz} + I_{21}u_{yz}] + \frac{1}{2}\left(\frac{t}{r_o}\right)^2 [I_{40}u_{xxz} + 2I_{31}u_{xyz} + I_{22}u_{yyz}]\right\}$$

$$\frac{\partial \phi_{20}}{\partial x} = -\frac{t^4}{r_o^3}\left\{I_{20}u_{xz} - \left(\frac{t}{r_o}\right)[I_{30}u_{xxz} + I_{21}u_{xyz}] + \frac{1}{2}\left(\frac{t}{r_o}\right)^2 [I_{40}u_{xxxz} + 2I_{31}u_{xxyz} + I_{22}u_{xyyz}]\right\} \qquad (73)$$

$$\frac{\partial \phi_{20}}{\partial y} = -\frac{t^4}{r_o^3}\left\{I_{20}u_{yz} - \left(\frac{t}{r_o}\right)[I_{30}u_{xyz} + I_{21}u_{yyz}] + \frac{1}{2}\left(\frac{t}{r_o}\right)^2 [I_{40}u_{xxyz} + 2I_{31}u_{xyyz} + I_{22}u_{yyyz}]\right\}$$

$$\frac{\partial \phi_{20}}{\partial z} = -\frac{t^4}{r_o^3}\left\{I_{20}u_{zz} - \left(\frac{t}{r_o}\right)[I_{30}u_{xzz} + I_{21}u_{yzz}] + \frac{1}{2}\left(\frac{t}{r_o}\right)^2 [I_{40}u_{xxzz} + 2I_{31}u_{xyzz} + I_{22}u_{yyzz}]\right\}$$

$$
\begin{aligned}
V_x^{(1x)} &= \frac{t^3}{r_o^2}\left\{I_{10}u_x - \left(\frac{t}{r_o}\right)[I_{20}u_{xx} + I_{11}u_{xy}] + \frac{1}{2}\left(\frac{t}{r_o}\right)^2[I_{30}u_{xxx} + 2I_{21}u_{xxy} \right. \\
&\qquad \left. + I_{12}u_{xyy}]\right\} \\
V_y^{(1x)} &= \frac{t^3}{r_o^2}\left\{I_{10}u_y - \left(\frac{t}{r_o}\right)[I_{20}u_{xy} + I_{11}u_{yy}] + \frac{1}{2}\left(\frac{t}{r_o}\right)^2[I_{30}u_{xxy} + 2I_{21}u_{xyy} \right. \\
&\qquad \left. + I_{12}u_{yyy}]\right\} \\
V_z^{(1x)} &= \frac{t^3}{r_o^2}\left\{I_{10}u_z - \left(\frac{t}{r_o}\right)[I_{20}u_{xz} + I_{11}u_{yz}] + \frac{1}{2}\left(\frac{t}{r_o}\right)^2[I_{30}u_{xxz} + 2I_{21}u_{xyz} \right. \\
&\qquad \left. + I_{12}u_{yyz}]\right\}
\end{aligned} \tag{74}
$$

$$
\begin{aligned}
V_x^{(1y)} &= \frac{t^3}{r_o^2}\left\{I_{01}u_x - \left(\frac{t}{r_o}\right)[I_{11}u_{xx} + I_{02}u_{xy}] + \frac{1}{2}\left(\frac{t}{r_o}\right)^2[I_{21}u_{xxx} + 2I_{12}u_{xxy} \right. \\
&\qquad \left. + I_{03}u_{xyy}]\right\} \\
V_y^{(1y)} &= \frac{t^3}{r_o^2}\left\{I_{01}u_y - \left(\frac{t}{r_o}\right)[I_{11}u_{xy} + I_{02}u_{yy}] + \frac{1}{2}\left(\frac{t}{r_o}\right)^2[I_{21}u_{xxy} + 2I_{12}u_{xyy} \right. \\
&\qquad \left. + I_{03}u_{yyy}]\right\} \\
V_z^{(1y)} &= \frac{t^3}{r_o^2}\left\{I_{01}u_z - \left(\frac{t}{r_o}\right)[I_{11}u_{xz} + I_{02}u_{yz}] + \frac{1}{2}\left(\frac{t}{r_o}\right)^2[I_{21}u_{xxz} + 2I_{12}u_{xyz} \right. \\
&\qquad \left. + I_{03}u_{yyz}]\right\}
\end{aligned} \tag{75}
$$

6.2.3 Far Field

As usual $\vec{n}$ denotes the unit normal vector to a projected flat panel and $\vec{i}_E$ and $\vec{j}_E$ are, respectively, unit vectors along the x- and y-axis of the panel coordinate system (equations (7.2.10) of reference 1). Define $\vec{r}_o$ as the vector from the origin of panel coordinates to the point where velocity is being evaluated and r_o as its magnitude. Certain auxiliary vectors are needed:

$$
\begin{aligned}
\vec{D} &= -\left[3\left(\frac{\vec{n}\cdot\vec{r}_o}{r_o}\right)\frac{\vec{r}_o}{r_o} - \vec{n}\right] \\
\vec{D}_i &= -\left[3\left(\frac{\vec{i}_E\cdot\vec{r}_o}{r_o}\right)\frac{\vec{r}_o}{r_o} - \vec{i}_E\right] \\
\vec{D}_j &= -\left[3\left(\frac{\vec{j}_E\cdot\vec{r}_o}{r_o}\right)\frac{\vec{r}_o}{r_o} - \vec{j}_E\right]
\end{aligned} \tag{76}
$$

The far-field expressions for the source velocities are

$$\vec{V}^{(0)} = \frac{t^2 I_{00}}{r_o^2} \frac{\vec{r}_o}{r_o} \tag{77}$$

$$\vec{V}^{(P)} = -\frac{t^4}{r_o^3} I_{20} \vec{D}$$

$$\vec{V}^{(Q)} = -\frac{t^4}{r_o^3} I_{11} \vec{D} \tag{78}$$

$$\vec{V}^{(R)} = -\frac{t^4}{r_o^3} I_{02} \vec{D}$$

$$\vec{V}^{(1x)} = \frac{t^3}{r_o^2} I_{10} \frac{\vec{r}_o}{r_o} - \frac{t^4}{r_o^3} [I_{20}\vec{D}_i + I_{11}\vec{D}_j]$$

$$\vec{V}^{(1y)} = \frac{t^3}{r_o^2} I_{01} \frac{\vec{r}_o}{r_o} - \frac{t^4}{r_o^3} [I_{11}\vec{D}_i + I_{02}\vec{D}_j] \tag{79}$$

The fact that three auxiliary vectors (76) are required means that in effect a transformation into panel coordinates has been performed. It appears to be somewhat faster computationally to use the vector far-field forms above rather than simply truncate the intermediate field formulas in panel coordinates. However, the advantage of the far-field formulas is reduced relative to that of reference 1, where only the vector $\vec{D}$ is required.

6.3 Vorticity Velocity Formulas

As defined in equation (59) the velocity due to a vorticity distribution on a panel is expressed as a sum of three terms which are denoted by superscripts 0, 1, and 2. The term with superscript 0 is the flat-panel constant-vorticity contribution. The other two terms account for surface curvature and vorticity derivative effects. Specific formulas are given below for these velocities in terms of surface curvatures P, Q and R and derivatives of the equivalent dipole distribution μ (section 5.3). Calculation of these quantities are described in subsequent sections. It is more convenient to group the formulas for each term of the velocity together

than to organize the formulas by Near-, Intermediate-, and Far-Fields, as is done for the source effects. As mentioned above, it is assumed that the formulas below are being evaluated in the panel coordinate system.

6.3.1 The Superscript Zero Velocity Components

It turns out that the super 0 components can be expressed in terms of the flat-panel constant-source velocities (equation (61)) as follows

$$\begin{aligned} V_{\omega x}^{(0)} &= -\mu_x V_z \text{ (source)} \\ V_{\omega y}^{(0)} &= -\mu_y V_z \text{ (source)} \\ V_{\omega z}^{(0)} &= \mu_x V_x \text{ (source)} - \mu_y V_y \text{ (source)} \end{aligned} \tag{80}$$

These are evaluated in the Near- and Intermediate-Fields by the formulas of reference 1 with the addition of first area moment terms in the Intermediate-Field as given in equation (70). In the Far-Field the first terms only of the Intermediate-Field formulas are retained, and this calculation is performed in panel coordinates.

6.3.2 The Superscript One Velocity Components

These components are as follows in the Near-Field:

$$\begin{aligned} V_{\omega x}^{(1)} &= -2(\mu_{xx}\phi_{10} + \mu_{xy}\phi_{01}) + \mu_x H + 2[(\mu_x Q - \mu_y P)(-J_{11} + xV_y \text{ (source)}) \\ &\quad + (\mu_x R - \mu_y Q)(-J_{02} + yV_y \text{ (source)})] \\ V_{\omega y}^{(1)} &= -2(\mu_{xy}\phi_{10} + \mu_{yy}\phi_{01}) + \mu_y H + 2[(-\mu_x Q + \mu_y P)(-J_{20} + xV_x \text{ (source)}) \\ &\quad + (-\mu_x R + \mu_y Q)(-J_{11} + yV_x \text{ (source)})] \\ V_{\omega z}^{(1)} &= 2[\mu_{xx}(-J_{20} + xV_x \text{ (source)}) + \mu_{yy}(-J_{02} + yV_y \text{ (source)}) \\ &\quad + \mu_{xy}(-2J_{11} + yV_x \text{ (source)} + xV_y \text{(source)})] \end{aligned} \tag{81}$$

where

$$H = P[J_{20} - 2xV_x \text{ (source)}] + 2Q[J_{11} - xV_y \text{ (source)} - yV_x \text{ (source)}] + R[J_{02} - 2yV_y \text{ (source)}] + h \tag{82}$$

and

$$h = \frac{1}{z}[Px^2 + 2Qxy + Ry^2]V_z \text{ (source)} \tag{83}$$

For small z, i.e., for points approaching the plane of the projected flat panel, there is a possible singularity in equation (83) due to the factor $1/z$. To avoid numerical difficulty a "small-z" test is employed and special procedures employed, if z is small. This is also required for the source formulas used in both the base method and the present method. The test and the procedures are described in section 7.8 of reference 1. In particular V_z (source) is set equal to zero if the projection (x,y) of the point into the plane of the panel lies outside the panel.

The procedure used for equation (83) uses the same small-z test as reference 1, and if it is satisfied sets

$$h = [Px^2 + 2Qxy + Ry^2]\frac{\partial \phi_{00}}{\partial z}, \quad (x,y) \text{ outside} \tag{84a}$$

$$= 0, \quad (x,y) \text{ inside} \tag{84b}$$

where the derivative of ϕ_{00} is given in equation (7.7.9) of reference 1. The reasoning that led to this choice is as follows. Since $V_z \to 0$ if (x,y) is outside, it is legitimate to use l'Hospital's rule on (83), and since $V_z = \phi_{00}$, equation (84a) follows. For (x,y) inside the panel the limit does not exist for arbitrary values of x and y. However, the assumption is made that if the point (x,y,z) approaches the panel it approaches along a line through the origin that does not lie in the xy-plane. Then the square bracket of (83) is $O(z^2)$ and (84b) follows. This assumption was made in the derivations of section 5.0. Furthermore, it is physically reasonable that if a point approaches a panel it does so at the panel control point (i.e., the origin), which is the only point where the normal-velocity boundary condition has been applied.

The formulas for the velocity components in the Intermediate Field are expressed in terms of the direction cosines α,β,γ which are defined in (7.6.2) of reference 1. In terms of the auxiliary potentials,

$$\phi^*_{pq} = \frac{1}{z}\phi_{pq} = \frac{t^{p+q+2}}{r_o^3}\left\{I_{pq} + 3\left(\frac{t}{r_o}\right)[\alpha I_{p+1,q} + \beta I_{p,q+1}] + \frac{3}{2}\left(\frac{t}{r_o}\right)^2[(5\alpha^2 - 1)I_{p+2,q} + 10\alpha\beta I_{p+1,q+1} + (5\beta^2 - 1)I_{p,q+2}]\right\} \tag{85}$$

the components in the Intermediate Field are

$$\begin{aligned}
V^{(1)}_{\omega x} &= -2z(\mu_{xx}\phi^*_{10} + \mu_{xy}\phi^*_{01}) + \mu_x H + 2[(\mu_x Q + \mu_y P)(y\phi^*_{10} - \phi^*_{11}) \\
&\qquad + (\mu_x R + \mu_y Q)(y\phi^*_{01} - \phi^*_{02})] \\
V^{(1)}_{\omega y} &= -2z(\mu_{xy}\phi^*_{10} + \mu_{yy}\phi^*_{01}) + \mu_y H + 2[(\mu_x Q + \mu_y P)(x\phi^*_{10} - \phi^*_{20}) \\
&\qquad + (\mu_x R + \mu_y Q)(x\phi^*_{01} - \phi^*_{11})] \\
V^{(1)}_{\omega z} &= 2[\mu_{xx}(x\phi^*_{10} - \phi^*_{20}) + \mu_{xy}\{(x\phi^*_{01} - \phi^*_{11}) + (y\phi^*_{10} - \phi^*_{11})\} + \mu_{yy}(y\phi^*_{01} - \phi^*_{02})]
\end{aligned} \tag{86}$$

where

$$H = P\phi^*_{20} + 2Q\phi^*_{11} + R\phi^*_{02} \tag{87}$$

The Far-Field calculation is obtained from (85) and (86) by truncating (85) with the first term containing even-ordered moments, i.e., the first term if $p+q$ is even, and the second term if $p+q$ is odd.

6.3.3 The Superscript Two Velocity Components

The superscript 2 velocity components are by far the most complicated analytically in the near field and a considerable number of secondary quantities must be defined. The auxiliary potentials ψ_{mn} are defined by

$$\psi_{mn} = 3z \iint_A \frac{(\xi - x)^m(\eta - y)^n}{r_f^5}\, d\xi d\eta \tag{88}$$

In terms of these potentials the near-field formulas are

$$\begin{aligned}
V^{(2)}_{\omega x} &= -z\mu_x V_{\omega R} \\
V^{(2)}_{\omega y} &= -z\mu_y V_{\omega R} \\
V_{\omega R} &= P\psi_{20} + 2Q\psi_{11} + R\psi_{02} + 2(xP + yQ)\psi_{10} + 2(xQ + yR)\psi_{01} \\
&\qquad + (Px^2 + 2Q_{xy} + Ry^2)\psi_{00}
\end{aligned} \tag{89}$$

and

$$V_{\omega z}^{(2)} = -\Big\{P\mu_x\psi_{30} + (2Q\mu_x + \mu_y P)\psi_{21} + (R\mu_x + 2Q\mu_y)\psi_{12} + R\mu_y\psi_{03} + 2(xP + yQ)\mu_x\psi_{20}$$
$$+ 2[(xQ + yR)\mu_x + (xP + yQ)\mu_y]\psi_{11} + 2(xQ + yR)\mu_y\psi_{02}$$
$$+ (Px^2 + 2Qxy + Ry^2)(\mu_x\psi_{10} + \mu_y\psi_{01})\Big\} \qquad (90)$$

To evaluate the ψ_{mn} the following quantities are defined

$$\begin{aligned}
q_{32} &= x - m_{32}y - b_{32} \\
q_{41} &= x - m_{41}y - b_{41} \\
e_{32} &= m_{32}q_{32} \\
e_{41} &= m_{41}q_{41} \\
f_{32} &= 1 + m_{32}^2 \\
f_{41} &= 1 + m_{41}^2 \\
E_{32} &= q_{32}^2 + f_{32}z^2 \\
E_{41} &= q_{41}^2 + f_{41}z^2 \\
g_{32} &= q_{32}^2 + z^2 \\
g_{41} &= q_{41}^2 + z^2
\end{aligned} \qquad (91)$$

$$\left.\begin{aligned}
h_m^{(1)} &= (y - \eta_1)^m \\
h_m^{(3)} &= (y - \eta_3)^m \\
a_m^{(1)} &= \frac{h_m^{(1)}}{(y - \eta_1)^2 + z^2} \\
a_m^{(3)} &= \frac{h_m^{(3)}}{(y - \eta_3)^2 + z^2}
\end{aligned}\right\} \quad m = 0,1 \qquad (92)$$

$$\left.\begin{aligned}
U_m^{(32)} &= \frac{1}{E_{32}}\left(\frac{a_m^{(1)}}{r_2} - \frac{a_m^{(3)}}{r_3}\right) \\
U_m^{(41)} &= \frac{1}{E_{41}}\left(\frac{a_m^{(1)}}{r_1} - \frac{a_m^{(3)}}{r_4}\right)
\end{aligned}\right\} \quad m = 0,1 \qquad (93)$$

$$\left.\begin{aligned} V_m^{(32)} &= \frac{1}{E_{32}}\left[\frac{h_m^{(1)}}{r_2} - \frac{h_m^{(3)}}{r_3}\right] \\ V_m^{(41)} &= \frac{1}{E_{41}}\left[\frac{h_m^{(1)}}{r_1} - \frac{h_m^{(3)}}{r_4}\right] \end{aligned}\right\} \quad m = 0,1 \tag{94}$$

$$\begin{aligned} W_m^{(32)} &= \frac{1}{E_{32}}\left(a_m^{(1)} r_2 - a_m^{(3)} r_3\right) \\ W_m^{(41)} &= \frac{1}{E_{41}}\left(a_m^{(1)} r_1 - a_m^{(3)} r_4\right) \end{aligned} \tag{95}$$

In terms of these, the ψ_{mn} are

$$\psi_{00} = z\Big\{[m_{32}W_0^{(32)} + q_{32}U_1^{(32)} - m_{32}z^2U_0^{(32)}] - [m_{41}W_0^{(41)} + q_{41}U_1^{(41)} - m_{41}z^2U_0^{(41)}]\Big\} + \frac{1}{z}[q_{32}W_1^{(32)} - q_{41}W_1^{(41)}] + \frac{1}{z^2}V_z \text{ (source)} \tag{96}$$

$$\psi_{01} = z\Big\{-m_{32}W_1^{(32)} + \frac{1}{f_{32}}[m_{32}e_{32}W_0^{(32)} + m_{32}(E_{32} + q_{32}^2)U_1^{(32)} + q_{32}g_{32}U_0^{(32)}] + m_{41}W_1^{(41)} - \frac{1}{f_{41}}[m_{41}e_{41}W_0^{(41)} + m_{41}(E_{41} + q_{41}^2)U_1^{(41)} + q_{41}g_{41}U_0^{(41)}]\Big\} \tag{97}$$

$$\psi_{10} = z[f_{32}V_1^{(32)} + e_{32}V_0^{(32)} - f_{41}V_1^{(41)} - e_{41}V_0^{(41)}] \tag{98}$$

$$\psi_{02} = z[q_{32}V_1^{(32)} - m_{32}z^2V_0^{(32)} - q_{41}V_1^{(41)} + m_{41}z^2V_0^{(41)}] - z^2\psi_{00} + 2V_z \text{ (source)} \tag{99}$$

$$\psi_{11} = z[e_{32}V_1^{(32)} + g_{32}V_0^{(32)} - e_{41}V_1^{(41)} - g_{41}V_0^{(41)}] \tag{100}$$

$$\psi_{20} = z[-q_{32}V_1^{(32)} + m_{32}z^2V_0^{(32)} + q_{41}V_1^{(41)} - m_{41}z^2V_0^{(41)}] + V_z \text{ (source)} \tag{101}$$

$$\psi_{03} = z\left\{\frac{1}{f_{32}}[m_{32}(E_{32} + q_{32}^2)V_1^{(32)} + q_{32}g_{32}V_0^{(32)}] - \frac{1}{f_{41}}[m_{41}(E_{41} + q_{41}^2)V_1^{(41)} + q_{41}g_{41}V_0^{(41)}] - z\psi_{01} + 2(L^{(12)} - L^{(34)}) - \frac{m_{32}}{(f_{32})^{3/2}}(3 + 2m_{32}^2)L^{(32)} + \frac{m_{41}}{(f_{41})^{3/2}}(3 + 2m_{41}^2)L^{(41)}\right\} \tag{102}$$

$$\psi_{12} = z\left\{\frac{1}{f_{32}}\left[(e_{32}^2 - E_{32})V_1^{(32)} + e_{32}g_{32}V_o^{(32)}\right] - \frac{1}{f_{41}}\left[(e_{41}^2 - E_{41})V_1^{(41)} + e_{41}g_{41}V_o^{(41)}\right] + \frac{1}{(f_{32})^{3/2}}L^{(32)} - \frac{1}{(f_{41})^{3/2}}L^{(41)}\right\} \quad (103)$$

$$\psi_{21} = z\left\{-\frac{1}{f_{32}}\left[m_{32}(q_{32}^2 + E_{32})V_1^{(32)} + q_{32}g_{32}V_o^{(32)}\right] + \frac{1}{f_{41}}\left[m_{41}(q_{41}^2 + E_{41})V_1^{(41)} + q_{41}g_{41}V_o^{(41)}\right] - \frac{m_{32}^3}{(f_{32})^{3/2}}L^{(32)} + \frac{m_{41}^3}{(f_{41})^{3/2}}L^{(41)} + L^{(12)} - L^{(34)}\right\} \quad (104)$$

$$\psi_{30} = z\left\{-\frac{1}{f_{32}}\left[(m_{32}^2E_{32} - q_{32}^2)V_1^{(32)} + e_{32}(E_{32} + z^2)V_o^{(32)}\right] + \frac{1}{f_{41}}\left[(m_{41}^2E_{41} - q_{41}^2)V_1^{(41)} + e_{41}(E_{41} + z^2)V_o^{(41)}\right] + \frac{2 + 3m_{32}^2}{(f_{32})^{3/2}}L^{(32)} - \frac{2 + 3m_{41}^2}{(f_{41})^{3/2}}L^{(41)}\right\} \quad (105)$$

A "small-z" test is required for ψ_{00} from (96). From (88) and (89) it can be seen that ψ_{00} occurs only when multiplied by a factor of $z(Px^2 + 2Qxy + Ry^2)$. Thus the 1/z term of ψ_{00} is not really singular, and the last term of ψ_{00} enters only in the combination (83) that gives h. Accordingly, the small-z procedure described in section 6.3.2 is used here as well.

Fortunately, the Intermediate-Field formulas for these components are quite simple. The auxiliary potentials Θ_{mn} are defined as suitably truncated expansions of the integrals

$$\iint_A \frac{\xi^m \eta^n}{r_f^5}\, d\xi d\eta$$

Specifically,

$$\Theta_{mn} = \frac{t^4}{r_o^5}\left\{I_{mn} + 5\frac{t}{r_o}\left[\alpha I_{m+1,n} + \beta I_{m,n+1}\right] + \frac{5}{2}\left(\frac{t}{r_o}\right)^2\left[(7\alpha^2 - 1)I_{m+2,n} + 14\alpha\beta I_{m+1,n+1} + (7\beta^2 - 1)I_{m,n+2}\right]\right\} \quad \text{for } m + n = 2 \quad (106a)$$

$$\theta_{mn} = \left(\frac{t}{r_o}\right)^5 \left\{ I_{mn} + 5 \left(\frac{t}{r_o}\right) [\alpha I_{m+1,n} + \beta I_{m,n+1}] \right\} \quad \text{for} \quad m + n = 3 \tag{106b}$$

and the components are

$$\begin{aligned} V_{\omega x}^{(2)} &= -z\mu_x V_{\omega R} \\ V_{\omega y}^{(2)} &= -z\mu_y V_{\omega R} \end{aligned} \tag{107}$$

where

$$V_{\omega R} = 3z(P\theta_{20} + 2Q\theta_{11} + R\theta_{02}) \tag{108}$$

and

$$V_{\omega z}^{(2)} = (x\mu_x + y\mu_y)V_{\omega R} - 3z[P\mu_x\theta_{30} + (2Q\mu_x + P\mu_y)\theta_{21} + (R\mu_x + 2Q\mu_y)\theta_{12} + R\mu_y\theta_{03}] \tag{109}$$

The Far-Field expressions are from equations (106) through (109) by truncating (106a) with the first term.

7.0 CALCULATION OF GEOMETRIC QUANTITIES FOR A PANEL

7.1 General Description of the Surface-Curvature Calculation

As illustrated in figure 1, the input to the program consists of coordinates of a set of points that define the body surface. The order of input is such that successive input points define a curve in the body surface called an N-line. When such a curve has been completely defined, the input logic notes the fact and subsequent points define an adjacent N-line. Four-cornered panels are formed from points on two adjacent N-lines and thus there is a "strip" of panels between adjacent N-lines (figure 1). Thus the ordering of surface panels is: all panels of one strip from first to last followed by all panels of the next strip, etc. This ordering of the panels is important both for the curvature calculation of this section and the source derivative calculation of section 8.1.

Suppose the geometric quantities for a typical panel are being calculated (the "panel in question" in figure 4). A least-square plane is computed for the four input points that form the corners of this panel in the manner described in references 1 and 2. A coordinate system, ξ,η,ζ, is constructed in this plane having the ζ-axis normal to the plane and having as origin the point whose coordinates are the averages of those of the four input points. The four input points are transformed into the ξ,η,ζ-coordinate system. Also transformed into this system are the additional input points that form the corners of the four panels adjacent to the one in question. As shown in figure 4, each adjacent panel provides two additional input points, because the other two are identical with two of those forming the corners of the panel in question. The expression defining the paraboloidal panel is assumed in the form

$$\zeta = z_o + A\xi + B\eta + P\xi^2 + 2Q\xi\eta + R\eta^2 \qquad (110)$$

The six parameters z_o, A, B, P, Q, and R are determined from: (a) requiring expression (110) to pass through the transformed corner points of the panel (four conditions), and (b) requiring expression (110) to agree as well as possible in a least squares sense with the eight additional input points for the adjacent panels. This last is performed with two independent parameters and thus represents two additional conditions — a total of six as

required. If the panel in question is the first or last of a strip, there are only three adjacent panels. This is also true for most panels on the first and last strips of a body. The first and last panels of the first and last strips have only two adjacent panels. Thus, there may be only six or four additional input points and the least-squares procedures are used accordingly. There is no difficulty since only two parameters are being adjusted. As described in the next section, it is necessary to perform this calculation in double-precision arithmetic.

It should be noted that the form (110) is not equivalent to the form (6) required by the derivations of section 5.0. This is because the least-square plane is not the plane of the flat projected panel. Rather the least-square plane is a temporary device needed to perform calculations. Once the form (110) has been obtained, the constant and linear terms are eliminated by translation and rotation of coordinates. The new plane obtained by these translations and rotations is that of the flat projected panel.

7.2 Specific Formulas for the Surface-Curvature Calculation

The initial portion of this calculation is identical with that of the flat-panel procedure of reference 1. Specifically, a "chord-plane" flat panel is constructed having the average point as origin and having the ζ axis in the normal direction as defined in reference 1. Equations (7.2.1) through (7.2.15) of reference 1 are carried out. Then the four input points used to form the panel are transformed into panel coordinates by the usual equations. Let ξ_K, η_K, ζ_K, K = 1, 2, 3, 4 denote the panel coordinates of the input points. The numbering is counterclockwise around the panel as viewed from the negative ζ-axis (figure 20 of reference 1). The following quantities are now defined.

$$d = \frac{1}{2}(\xi_3 - \xi_4) \qquad e = \frac{1}{2}(\xi_2 - \xi_1)$$

$$q = \frac{1}{4}(\xi_1 + \xi_2 - \xi_3 - \xi_4)$$

$$h = \frac{1}{4}(\eta_1 + \eta_2 - \eta_3 - \eta_4) \tag{111}$$

$$\varepsilon = \frac{1}{4}(\eta_1 - \eta_2 + \eta_3 - \eta_4)$$

$$f = \frac{1}{4}(\zeta_1 - \zeta_2 + \zeta_3 - \zeta_4)$$

Then necessary derived quantities are

$$z_P = -\frac{1}{2}(d^2 + e^2 + 2q^2)$$

$$z_Q = -\varepsilon(d - e) - 2qh$$

$$z_R = -(h^2 + \varepsilon^2)$$

$$Q_o = -\frac{f}{h(d + e)}$$

$$Q_A = \frac{d - e}{2h(d + e)}$$

$$Q_B = \frac{\varepsilon}{h(d + e)}$$

$$Q_P = -\frac{q}{h}$$

$$C_{AA} = \frac{1}{d + e}\left[2de - \frac{q\varepsilon(d - e)}{h}\right] \qquad (112)$$

$$C_{AB} = \frac{e - d}{e + d}\varepsilon$$

$$D_o = f\frac{e - d}{e + d}$$

$$D_R = 2h\varepsilon$$

$$C_{BA} = 2q + \frac{(e - d)\varepsilon}{h}$$

$$C_{BB} = \frac{2}{h}(h^2 - \varepsilon^2)$$

$$E_o = -\frac{2\varepsilon}{h}f$$

$$E_P = d^2 - e^2$$

A 2 x 2 set of linear equations is solved for three different right sides to obtain the quantities A_o, B_o, A_R, B_R, A_P, B_P, namely

$$C_{AA}A_o + C_{AB}B_o = D_o \qquad (113a)$$

$$C_{BA}A_o + C_{BB}B_o = E_o$$

$$C_{AA}A_R + C_{AB}B_R = D_R \qquad (113b)$$

$$C_{BA}A_R + C_{BB}B_R = 0$$

$$C_{AA}A_P + C_{AB}B_P = 0$$
$$C_{BA}A_P + C_{BB}B_P = E_P \qquad (113c)$$

Now if the quantities A, B, Q and z_o in (110) are taken in the form

$$A = A_o + A_P P + A_R R$$
$$B = B_o + B_P P + B_R R$$
$$Q = Q_o + Q_A A + Q_B B + Q_P P \qquad (114)$$
$$z_o = z_P P + z_Q Q + z_R R$$

then expression (110) passes through the input points ξ_K, η_K, ζ_K, K = 1,2,3,4 for arbitrary values of P and R. These two quantities are adjusted to give a least-square fit to the surrounding panels.

If the quantities A, B, Q and z_o are replaced in (110) by their representations in (114), the result is

$$\zeta = D(\xi,\eta) + E(\xi,\eta)P + F(\xi,\eta)R \qquad (115)$$

where

$$D(\xi,\eta) = z_Q(Q_o + Q_A A_o + Q_B B_o) + A_o\xi + B_o\eta + (2Q_o + 2Q_A A_o + 2Q_B B_o)\xi\eta$$
$$E(\xi,\eta) = z_P + z_Q(Q_A A_P + Q_B B_P + Q_P) + A_P\xi + B_P\eta + \xi^2 + (2Q_A A_P + 2Q_B B_P + 2Q_P)\xi\eta \qquad (116)$$
$$F(\xi,\eta) = z_Q(Q_A A_R + Q_B B_R) + z_R + A_R\xi + B_R\eta + \eta^2 + (2Q_A A_R + 2Q_B B_R)\xi\eta$$

Figure 4 shows the four panels surrounding the "panel in question" whose geometry is being calculated. For the interior panel shown, the four surrounding panels are defined by a total of eight input points that are not also input points defining the panel in question. As detailed in section 7.1, panels at the edge of a section may have 2 or 3 adjacent panels, which correspondingly may have 4 or 6 input points. The input points of the surrounding panels are transformed into the coordinate system of the panel in question. The resulting coordinates are ξ_m, η_m, ζ_m, m = 1, ..., 8 (or 6 or 4). The least-square procedure is accomplished by defining the quantities

$$C_{RR} = \sum_{m=1}^{8} [F(\xi_m,\eta_m)]^2$$

$$C_{PP} = \sum_{m=1}^{8} [E(\xi_m,\eta_m)]^2$$

$$C_{RP} = C_{PR} = \sum_{m=1}^{8} E(\xi_m,\eta_m)F(\xi_m,\eta_m) \qquad (117)$$

$$L_1 = \sum_{m=1}^{8} [\zeta_m - D(\xi_m,\eta_m)]F(\xi_m,\eta_m)$$

$$L_2 = \sum_{m=1}^{8} [\zeta_m - D(\xi_m,\eta_m)]E(\xi_m,\eta_m)$$

after which P and R are solved for from the 2×2 system of equations

$$C_{RR}R + C_{RP}P = L_1$$
$$C_{PR}R + C_{PP}P = L_2 \qquad (118)$$

If the panel in question is on the edge of a section, the summations in (117) extend to 4 or 6 as appropriate rather than to 8. It was found that on wings where panel aspect ratios of 50 are not uncommon, the fact that four of the points (ξ_m,η_m,ζ_m) have much larger $\xi\eta$ coordinates than the other four can lead to ill-conditioning of equations (118) due to round-off error. Accordingly, equations (117) and (118) are calculated using double-precision arithmetic.

Once P and R are known, all other parameters of (110) can be obtained from (114).

If one side of the panel is much smaller than the other, some instability can result in equations (111), (112), and (113). Accordingly, in this case special "zero length side" formulas are used:

$$f = \varepsilon = 0$$
$$A_o = A_R = A_P = 0 \qquad (119)$$
$$B_o = B_R = 0$$

$$B_P = \frac{d^2 - e^2}{2h}$$

7.3 General Description of the Calculation of the Control Point and the Projected Panel

All of the calculations of sections 7.1 and 7.2 are carried out in a coordinate system whose $\xi\eta$-plane is the "chord plane", which is also the plane of the flat panel of reference 1. However, this is not the plane of the projected flat panel of the present method as described in section 5.0. Among other things the projected flat panel is tangent to the true curved surface. The tangency point is both the control point of the panel and the origin of the panel coordinate system. It remains to compute the tangency point, the normal direction at the tangency point, and the geometric quantities associated with the flat projected panel. These quantities may be defined in several ways, all of which are equivalent to the order of accuracy of the overall calculation. The selections made for the present method are outlined below.

The control point is taken as that point of the surface (110) that is nearest the origin, and the normal direction is that from the origin to this nearest point. Thus, to the order of accuracy being considered, the control point is the point on the true curved surface nearest the average point of the four input corner points. The size and shape of the projected flat panel are assumed identical to those of the "chord plane" flat panel calculated by the procedure of reference 1. Thus the flat projected panel is determined solely by the coordinates of the control point and the unit vectors defining the axes of the panel coordinate system, whose ζ-axis defines the normal direction.

7.4 Specific Formulas for the Calculation of the Control Point and the Projected Panel

The derivatives of expression (110) are

$$\begin{aligned} \zeta_\xi &= A + 2(P\xi + Q\eta) \\ \zeta_\eta &= B + 2(Q\xi + R\eta) \end{aligned} \tag{120}$$

The point on the surface nearest the origin is characterized by the condition that the vector from the origin is parallel to the local normal vector, or

$$[\xi\vec{i} + \eta\vec{j} + \zeta(\xi,\eta)\vec{k}] \times [-\zeta_\xi\vec{i} - \zeta_\eta\vec{j} + \vec{k}] = 0 \tag{121}$$

This last is equivalent to the two scalar equations

$$G(\xi,\eta) = \xi + \zeta(\xi,\eta)\zeta_\xi(\xi,\eta) = 0$$
$$H(\xi,\eta) = \eta + \zeta(\xi,\eta)\zeta_\eta(\xi,\eta) = 0 \tag{122}$$

The nonlinear equations (122) are solved by Newton-Raphson iteration. The derivatives are

$$G_\xi = 1 + \zeta_\xi^2 + 2P\zeta$$
$$G_\eta = H_\xi = \zeta_\xi\zeta_\eta + 2Q\zeta \tag{123}$$
$$H_\eta = 1 + \zeta_\eta^2 + 2R\zeta$$

Let ξ_k,η_k denote the approximations to the solutions of (122) obtained in the k-th iteration. The next approximation is obtained by solving the 2 x 2 set of linear equations

$$G_\xi(\xi_k,\eta_k)(\xi_{k+1} - \xi_k) + G_\eta(\xi_k,\eta_k)(\eta_{k+1} - \eta_k) = -G(\xi_k,\eta_k)$$
$$H_\xi(\xi_k,\eta_k)(\xi_{k+1} - \xi_k) + H_\eta(\xi_k,\eta_k)(\eta_{k+1} - \eta_k) = -H(\xi_k,\eta_k) \tag{124}$$

Initial values are taken as $\xi_0 = \eta_0 = 0$. The iteration converges very rapidly to the nearest point with coordinates $\xi_\infty,\eta_\infty,\zeta_\infty$. The local normal vector at this point (which, of course, is parallel to the vector from the origin) has components $\gamma_1,\gamma_2,\gamma_3$ in this coordinate system, where

$$\gamma_1 = -\zeta_\xi(\xi_\infty,\eta_\infty)/\gamma$$
$$\gamma_2 = -\zeta_\eta(\xi_\infty,\eta_\infty)/\gamma \tag{125}$$
$$\gamma_3 = \sqrt{1 - \gamma_1^2 - \gamma_2^2}$$

and

$$\gamma = \sqrt{1 + \zeta_\xi^2 + \zeta_\eta^2} \tag{126}$$

The above vector is the unit normal vector to the projected flat panel and defines the third axis of its coordinate system. It is now necessary to construct unit vectors parallel to the other two axes of this system. Preliminary quantities are

$$\overline{\gamma_1} = \gamma_1/\sqrt{\gamma_1^2 + \gamma_2^2}, \qquad \overline{\gamma_2} = \gamma_2/\sqrt{\gamma_1^2 + \gamma_2^2} \tag{127}$$

If both γ_1 and γ_2 are essentially zero, set $\overline{\gamma_1} = \overline{\gamma_2} = \sqrt{2}/2$. The components of the vector parallel to the first axis of the projected flat panel's coordinate system are $\alpha_1, \alpha_2, \alpha_3$ where

$$\alpha_1 = (\overline{\gamma}_2)^2 + \gamma_3(\overline{\gamma}_1^2)$$

$$\alpha_2 = (\gamma_3 - 1)\overline{\gamma}_1\overline{\gamma}_2 \tag{128}$$

$$\alpha_3 = -\overline{\gamma}_1\sqrt{1 - \gamma_3^2}$$

Finally, the components $\beta_1, \beta_2, \beta_3$ of the unit vector parallel to the second coordinate axis are obtained by taking the cross product of the vector (125) and the vector (128). The matrix

$$[A] = \begin{bmatrix} \alpha_1 & \alpha_2 & \alpha_3 \\ \beta_1 & \beta_2 & \beta_3 \\ \gamma_1 & \gamma_2 & \gamma_3 \end{bmatrix} \tag{129}$$

would thus be suitable for transforming vectors and points between the coordinate systems of the projected flat panel and the "chord-plane" panel. As defined in equation (7.2.10) of reference 1, the transformation matrix of the "chord-plane" panel is.

$$[a(old)] = \begin{bmatrix} a_{11} & a_{12} & a_{13} \\ a_{21} & a_{22} & a_{23} \\ a_{31} & a_{32} & a_{33} \end{bmatrix} \tag{130}$$

Thus the transformation matrix for the projected flat panel is obtained as the matrix product

$$[a(new)] = [A]\ [a(old)] \tag{131}$$

The rows of matrix (131) are unit vectors parallel to the axes of the coordinate system of the projected flat panel expressed in the reference coordinate system. In particular, the third row is the normal vector. This matrix is used in the manner of reference 1 to transform points and vectors.

The reference coordinates of the control point are obtained from

$$
\begin{aligned}
x_o &= x_{av} + a_{11}\xi_\infty + a_{21}\eta_\infty + a_{31}\zeta_\infty \\
y_o &= y_{av} + a_{12}\xi_\infty + a_{22}\eta_\infty + a_{32}\zeta_\infty \\
z_o &= z_{av} + a_{13}\xi_\infty + a_{23}\eta_\infty + a_{33}\zeta_\infty
\end{aligned}
\tag{132}
$$

The quantities on the right side of (132) are those of (130) not (131). However, this is the last use of matrix (130) which is now discarded in favor of (131) just as the average point (x_{av}, y_{av}, z_{av}) is discarded in favor of (x_o, y_o, z_o). Because of the way the projected flat panel has been defined, these are the only required replacements. All other quantities that have been computed for the "chord-plane" panel are valid also for the projected flat panel, specifically the slopes and corner-point coordinates, equations (7.2.12) and (7.2.15) of reference 1. The remaining geometric quantities of the projected flat panel are calculated in the manner of reference 1 beginning with equation (7.2.20).

It could be argued that the entire process of section 7.0 could be iterated. Using the new panel coordinate system, the procedure of sections 7.1 and 7.2 would give somewhat different values of the coefficients in (110) which could in turn be used in the calculation of the present section. However, if panel dimensions are small compared to physical dimensions of the body, as is assumed throughout the present method, ζ is small everywhere on the panel and the rotations implied by matrix (129) are also small. It can be shown that the changes to be realized by iteration are of higher (third) order in panel dimensions, and it is consistent with the other approximations that have been made not to iterate. This course has been adopted for simplicity.

8.0 THE SOURCE DERIVATIVE TERMS. ASSEMBLY OF THE MATRIX OF INFLUENCE COEFFICIENTS

8.1 The Least-Square Procedure. Geometric Constants

As stated in section 6.2, the basic source velocity formula (60) contains coefficients σ_x and σ_y, which are the derivatives of the source density with respect to the panel's coordinate directions. It is not intended that these be additional unknowns. Instead, they are expressed in terms of the unknown values of source density at the control points of the surrounding panels. Thus, ultimately the values of source density at the control points of the panels are the only unknowns. Just as for the curvature calculation of section 7.1, the source-derivative procedure is slightly different for the first and last panels of a strip and for panels of the first and last strips. However, the modifications are quite straightforward. In the initial discussion it is assumed that the panel on which source derivatives are being evaluated (the panel in question) has adjacent panels on all four sides as shown in figure 5. For the purposes of the present discussion only, the control points of the adjacent panels are numbered $K = 0, 1, 2, 3, 4$ as shown in figure 5, where 0 denotes the element in question. These control points are transformed into the coordinate system of the panel in question. Let the ξ and η coordinates of these control points be ξ_{0K}, η_{0K}, $K = 0, 1, \ldots, 4$ and the values of source density at the control points be σ_K, $K = 0, 1, \ldots, 4$ (evidently $\xi_{00} = \eta_{00} = 0$). The source density on the panel in question is assumed in the form

$$\sigma(\xi,\eta) = \sigma_0 + \sigma_x\xi + \sigma_y\eta \tag{133}$$

This is fitted in a least-square sense to the values of source density at the control points of the adjacent panels. That is, the source density variation on the panel in question is a least-square plane through neighboring values. This process expresses the source derivatives on the panel in question in terms of the unknown values of source density on the adjacent panels in the form

$$\sigma_x = \sum_{K=0}^{4} c_K^{(x)}\sigma_K$$

$$\sigma_y = \sum_{K=0}^{4} c_K^{(y)} \sigma_K \tag{134}$$

where the coefficients $c_K^{(x)}$ and $c_K^{(y)}$ are purely geometrical.

Specifically, let M be the number of control points involved in the least-square fit. Thus $M = 5$ for an interior panel as shown in Figure 5, but $M = 4$ for most panels of the first and last strips and for the first and last panels of interior strips. For the first and last panels of the first and last strips $M = 3$. The following quantities are defined

$$X = \sum_{K=0}^{M-1} \xi_{0K} \quad , \quad Y = \sum_{K=0}^{M-1} \eta_{0K}$$

$$S = \sum_{K=0}^{M-1} \xi_{0K}^2 \quad , \quad T = \sum_{K=0}^{M-1} \xi_{0K}\eta_{0K} \quad , \quad U = \sum_{K=0}^{M-1} \eta_{0K}^2 \tag{135}$$

$$a = S - \frac{X^2}{M} \quad , \quad b = T - \frac{XY}{M} \quad , \quad c = U - \frac{Y^2}{M}$$

$$d = ac - b^2$$

Then the desired coefficients are

$$c_K^{(x)} = \frac{c}{d}\xi_{0K} - \frac{b}{d}\eta_{0K} + \frac{b}{c}\frac{Y}{M} - \frac{c}{d}\frac{X}{M}$$

$$c_K^{(y)} = -\frac{b}{d}\xi_{0K} + \frac{a}{d}\eta_{0K} + \frac{b}{d}\frac{X}{M} - \frac{a}{d}\frac{Y}{M} \qquad K = 0, 1, \ldots, M \tag{136}$$

There are 2M "source derivative coefficients," a total of 10 for an interior panel. These are calculated once and for all and stored with the other geometric quantities defining each panel.

8.2 Logic of the Assembly Procedure

In the base method the velocity induced by a panel depends only on the source density on that panel and thus the "influence coefficients" for that panel are calculated solely from that panel's geometry. The essentially new feature of the source derivative procedure is that the velocity induced by a

panel depends on the value of source density at the control point of that panel and also on the values of source density at the control points of adjacent elements. Similarly, the velocities induced by adjacent elements depend on the source density on the panel in question. Thus the "influence coefficients" for a panel depend not only on the geometry of that panel but also on the geometry of adjacent panels and the assembly of the influence coefficient matrix is more complicated.

Let the panels be numbered consecutively in the order they have been formed. Thus, reference is made to the i-th panel and to the j-th panel where both i and j range from 1 to N. Another way of stating the essentially new feature above is that a distinction must be made between the effect of the j-th panel and the effect of the j-th value of source density, whereas these two effects are identical in the base method. Let $\vec{V}^*_{ij}$ be the velocity induced at the i-th control point by the j-th panel and $\vec{V}_{ij}$ be the velocity induced at that point by the j-th value of source density. Then in the notation of section 6.2 and the present section,

$$\vec{V}^*_{ij} = [\vec{V}^{(0)} + \vec{V}^{(P)}P + 2\vec{V}^{(Q)}Q + \vec{V}^{(R)}R + c_o^{(x)}\vec{V}^{(1x)} + c_o^{(y)}\vec{V}^{(1y)}]\sigma_o + \sum_{K=1}^{M-1} [c_K^{(x)}\vec{V}^{(1x)} + c_K^{(y)}\vec{V}^{(1y)}]\sigma_K \qquad (137)$$

Notice that subscripts i and j are omitted on the right side of equation (137) for simplicity. In the overall numbering scheme, σ_o in (137) is σ_j and σ_1, σ_2, σ_3, and σ_4 have subscripts near j. All velocities in (137) depend only on the geometry of the j-th panel. The curvatures P, Q, R and the coefficients $c_K^{(x)}$ and $c_K^{(y)}$ depend on the surrounding panels, but once calculated they can be associated with the j-th panel only.

Consider now the i-th row of the matrix $\vec{V}_{ij}$, which expresses the effects of the various values of source density at the i-th control point. The first bracketed term in (137) is an effect of σ_j and is added to the j-th location of the row. The four terms in the summation of (137) represent effects of other values of σ and must be added to other locations. Referring to figure 5, it can be seen that the panels numbered 1 and 2 are on the same strip as the panel in question and thus represent effects of the preceeding and succeeding values of σ. In particular, value 1 is associated with

σ_{j-1} and value 2 with σ_{j+1} and the relevant terms of (137) are added to those locations. Panels 3 and 4, however, are on adjacent strips. Suppose there are E panels on each strip. Then value 3 is associated with σ_{j-E} and value 4 with σ_{j+E}, and the relevant terms of (137) are added to these locations of the row.

If the matrix of influence coefficients was formed row by row, or if it could be completely contained in high-speed storage, the above procedure would be fairly simple (as indeed it is in two dimensions). However, the matrix is formed column by column, and some rather complicated logic is required. By retaining always three columns of the matrix in high-speed storage, the terms in (137) that belong in columns j-1, j, and j+1 can be put into the proper locations immediately and the results stored on the main matrix tape (or disk) in the usual way. However, the j-E effects must be stored on a second tape (or disk) and the j+E effects on a third tape. Thus, when the usual calculation is over and all values of j have been considered, the result is three tapes each containing an almost full matrix. (The only deviations from full matrices are that the matrix on the second tape has zeros in the last E columns and that on the third tape has zeros in the first E columns.) The three matrices are brought into high-speed storage column by column, and corresponding columns are added location by location to produce the final $\vec{V}_{ij}$ matrix. To save time the induced normal velocity matrix is also computed at this time by taking dot products with the unit normal vectors to the panels.

9.0 THE GLOBAL VORTICITY VARIATION

9.1 General Description of the Procedure

The formulas of section 6.3 give velocity components at a point due to a vorticity distribution on a curved panel in terms of the first and second derivatives of the equivalent dipole distribution $\mu(\xi,\eta)$ evaluated at the panel "center," i.e., the origin of panel coordinates. Thus there are five parameters per panel, μ_x, μ_y, μ_{xx}, μ_{xy}, μ_{yy}, and these permit a general quadratic dipole variation. These derivatives are determined by the algorithm adopted for global vorticity or dipole variation.

As mentioned in section 4.0, vorticity is an auxiliary singularity in the present method, and its main purpose is to satisfy the Kutta condition along a wing trailing edge. Thus a global variation algorithm is chosen that expresses the vorticity distribution over the entire body (or the equivalent dipole distribution) in terms of a number of parameters equal to the number of trailing-edge segments at which the Kutta condition is applied (figure 1). In the logical scheme of the present method there are three aspects to the global variation: (1) global variation along an N-line (figure 1), (2) local variation along an N-line over a single panel, and (3) local variation between consecutive N-lines across the intervening strip of panels. The global variation across the N-lines ("spanwise") is not part of the global variation algorithm but is determined by the Kutta condition.

The global variation along an N-line is the most basic assumption and the one that permits the most flexibility. The distribution of the equivalent dipole strength is taken as a particular monotonic function of arc length along the N-line, beginning at the trailing edge, coming forward to the leading edge along the lower surface, proceeding along the upper surface back to the trailing edge, and continuing into the wake. Section 7.3 of reference 1 gives a very complete description, which, while it is specialized to the case of a particular distribution function, illustrates the general case very well. (As discussed there the N-line may be traversed in the opposite sense also, i.e., upper surface first.) It is understood that the actual variation of equivalent dipole strength along the N-line is the product of the distribution function and an initially unknown multiplicative constant whose value is a measure of the local "bound" vorticity strength. Values of the multiplicative

constants on all N-lines are obtained as solutions of the simultaneous equations that express the Kutta condition at the trailing-edge segments of the strips (reference 1 and section 10.0). In the usual case the equivalent dipole strength on the wake portion of the N-line is taken as constant and equal to its value at the upper surface trailing edge. As described in the paper form of reference 1, the base method has two options for the global dipole variation along an N-line: linear and cubic, which correspond, respectively, to a constant and a parabolic "chordwise" variation of bound vorticity.

Contradictory as it may first appear, the assumptions of the global variation algorithm also determine the local variation over a panel of the vorticity or dipole strength. Since the formulas of section 6.3 permit a linear vorticity variation (quadratic dipole variation), no higher-order variation can be considered. On the other hand, that order of variation should be used to obtain the full power of the present method. In the base method of reference 1, the dipole variation over the "chord" of the panel is linear, while its "spanwise" variation may be either constant, linear, or quadratic.

Because only a limited amount of effort could be devoted to a preliminary version of the present method, it was decided to employ the global variation algorithm of the base method of reference 1 (including the refinements of the paper version), even though some of the capability would not be utilized. It is intended to develop a more sophisticated algorithm at some future time.

9.2 Formulas for Constant Chordwise Vorticity

In this option, the equivalent dipole strength μ is assumed to vary linearly along an N-line in the form

$$\mu = Bs \tag{138}$$

where B is the unknown multiplicative parameter and s is arc length measured from the trailing edge. Over an individual panel the variation is

$$\mu = A + B\xi = B(h + \xi) \tag{139}$$

where ξ has its usual meaning as a panel coordinate (figure 20 of reference 1) and h is the total arc length along the N-line up to the η-axis ($\xi = 0$) of panel coordinates. The two N-lines bounding the panel are denoted the

"first" and the "second" and quantities associated with them are identified by subscripts F and S, respectively. Then the dipole strength on the panel is (compare equation (7.3.7) of reference 1)

$$\mu = \frac{B_F - B_S}{w}\xi\eta + \frac{B_F h_F - B_S h_S}{w}\eta + \frac{B_S\eta_1 - B_F\eta_3}{w}\xi + \frac{B_S h_S \eta_1 - B_F h_F \eta_3}{w} + c(B_F - B_S)(\eta - \eta_3)(\eta - \eta_1) + d(B_F - B_S)\xi^2 \tag{140}$$

where w is the panel width and η_1 and η_3 are, respectively, the η-coordinates of the first and second N-lines. By comparison with equation (50) of section 5.3 the above gives the required five parameters as

$$\mu_x = \frac{B_S\eta_1 - B_F\eta_3}{w}$$

$$\mu_y = \frac{B_F h_F - B_S h_S}{w} - c(B_F - B_S)(\eta_1 + \eta_3) \tag{141}$$

$$\mu_{xx} = d(B_F - B_S)$$

$$\mu_{xy} = \frac{1}{2}\frac{B_F - B_S}{w}$$

$$\mu_{yy} = c(B_F - B_S)$$

For future applications provision has been made for the constants c and d for each panel, but in the current form of the present method d is always zero and c is nonzero only on wake panels as explained in reference 1.

From (140) it is clear that the equivalent dipole distribution has the form

$$\mu = B_F\mu_F + B_S\mu_S \tag{142}$$

where μ_F and μ_S are independent of the values of B and can be obtained directly from (140). In particular μ_F is a dipole distribution that is zero on the second N-line and has a unit derivative on the first. The velocity due to the vorticity distribution on the panel also can be written

$$\vec{V}_\omega = \vec{V}_\omega(F)\mu_F + \vec{V}_\omega(S)\mu_S \tag{143}$$

where the velocities $\vec{V}_\omega(F)$ and $\vec{V}_\omega(S)$ correspond, respectively, to equivalent dipole distributions μ_F and μ_S. As in equation (59) of section 5.3, each

of these two velocities is the sum of three terms

$$\begin{aligned}\vec{V}_\omega(F) &= \vec{V}_\omega^{(0)}(F) + \vec{V}_\omega^{(1)}(F) + \vec{V}_\omega^{(2)}(F)\\ \vec{V}_\omega(S) &= \vec{V}_\omega^{(0)}(S) + \vec{V}_\omega^{(1)}(S) + \vec{V}_\omega^{(2)}(S)\end{aligned} \tag{144}$$

Specific assembly formulas for the components of the velocities in (144) are given below.

9.2.1 Near-Field Formulas for Panels on the Body

The superscript zero components are

$$\begin{aligned}V_{\omega x}^{(0)}(S) &= -\frac{n_1}{w} V_z \text{ (source)}\\ V_{\omega x}^{(0)}(F) &= \frac{n_3}{w} V_z \text{ (source)}\\ V_{\omega y}^{(0)}(S) &= \left[\frac{h_S}{w} - c(n_1 + n_3)\right] V_z \text{ (source)}\\ V_{\omega y}^{(0)}(F) &= -\left[\frac{h_F}{w} - c(n_1 + n_3)\right] V_z \text{ (source)}\\ V_{\omega z}^{(0)}(S) &= \frac{n_1}{w} V_x \text{ (source)} - \left[\frac{h_S}{w} - c(n_1 + n_3)\right] V_y \text{ (source)}\\ V_{\omega z}^{(0)}(F) &= -\frac{n_3}{w} V_x \text{ (source)} + \left[\frac{h_F}{w} - c(n_1 + n_3)\right] V_y \text{ (source)}\end{aligned} \tag{145}$$

where all quantities on the right have their usual meanings. Near-field formulas are (7.7.7) of reference 1.

Define auxiliary quantities by

$$\begin{aligned}J_1^* &= -J_{20} + xV_x \text{ (source)}\\ J_2^* &= -J_{11} + xV_y \text{ (source)}\\ J_3^* &= -J_{11} + yV_x \text{ (source)}\\ J_4^* &= -J_{02} + yV_y \text{ (source)}\end{aligned} \tag{146a}$$

The J_{mn} have the meanings appropriate to the source formulas. Specifically, J_{20} is given by equation (64), J_{11} by (7.7.12) of reference 1, and J_{02} by

$$J_{02} = H_{02} - zV_z \text{ (source)} \tag{146b}$$

where H_{02} is given by (7.7.15) of reference 1.

In terms of these, the superscript one components are

$$\begin{aligned}
V^{(1)}_{\omega x}(S) &= 2(d\phi_{10} + \frac{1}{2w}\phi_{01}) + \frac{\eta_1}{w}H + 2\frac{\eta_1}{w}(QJ_2^* + RJ_4^*) \\
&\quad + 2\left[\frac{h_S}{w} - c(\eta_1 + \eta_3)\right](PJ_2^* + QJ_4^*) \\
V^{(1)}_{\omega x}(F) &= -2(d\phi_{10} + \frac{1}{2w}\phi_{01}) - \frac{\eta_3}{w}H - 2\frac{\eta_3}{w}(QJ_2^* + RJ_4^*) \\
&\quad - 2\left[\frac{h_F}{w} - c(\eta_1 + \eta_3)\right](PJ_2^* + QJ_4^*) \\
V^{(1)}_{\omega y}(S) &= 2\left(\frac{1}{2w}\phi_{10} + c\phi_{01}\right) - 2\frac{\eta_1}{w}(QJ_1^* + RJ_3^*) \\
&\quad - \left[\frac{h_S}{w} - c(\eta_1 + \eta_3)\right](H + 2PJ_1^* + 2QJ_3^*) \\
V^{(1)}_{\omega y}(F) &= -2\left(\frac{1}{2w}\phi_{10} + c\phi_{01}\right) + 2\frac{\eta_3}{w}(QJ_1^* + RJ_3^*) \\
&\quad + \left[\frac{h_F}{w} - c(\eta_1 + \eta_3)\right](H + 2PJ_1^* + 2QJ_3^*) \\
V^{(1)}_{\omega z}(S) &= -2[dJ_1^* + cJ_4^* + \frac{1}{2w}(J_2^* + J_3^*)] \\
V^{(1)}_{\omega z}(F) &= 2[dJ_1^* + cJ_4^* + \frac{1}{2w}(J_2^* + J_3^*)]
\end{aligned} \tag{147}$$

where H is defined by (82).

In the evaluation of the superscript, two components, $V_{\omega R}$ is given by (89), and (90) is decomposed into

$$V^{(2)}_{\omega z} = \mu_x w_{xz} + \mu_y w_{yz} \tag{148}$$

so that

$$\begin{aligned}
w_{xz} &= P\psi_{30} + 2Q\psi_{21} + R\psi_{12} + 2(xP + yQ)\psi_{20} + 2(xQ + yR)\psi_{11} \\
&\quad + (Px^2 + 2Qxy + Ry^2)\psi_{10} \\
w_{yz} &= P\psi_{21} + 2Q\psi_{12} + R\psi_{03} + 2(xP + yQ)\psi_{11} + 2(xQ + yR)\psi_{02} \\
&\quad + (Px^2 + 2Qxy + Ry^2)\psi_{01}
\end{aligned} \tag{149}$$

The ψ_{mn} are defined by equations (96) through (105). Then

$$V^{(2)}_{\omega x}(S) = -z\frac{\eta_1}{w}V_{\omega R} \qquad V^{(2)}_{\omega x}(F) = z\frac{\eta_3}{w}V_{\omega R} \tag{150}$$

$$
\begin{aligned}
V^{(2)}_{\omega y}(S) &= z\left[\frac{h_S}{w} - c(\eta_1 + \eta_3)\right] V_{\omega R} \\
V^{(2)}_{\omega y}(F) &= -z\left[\frac{h_F}{w} - c(\eta_1 + \eta_3)\right] V_{\omega R} \\
V^{(2)}_{\omega z}(S) &= -\frac{\eta_1}{w} w_{xz} + \left[\frac{h_S}{w} - c(\eta_1 + \eta_3)\right] w_{yz} \\
V^{(2)}_{\omega z}(F) &= \frac{\eta_3}{w} w_{xz} - \left[\frac{h_F}{w} - c(\eta_1 + \eta_3)\right] w_{yz}
\end{aligned}
\tag{150}
$$

9.2.2 Changes in On-Body Panel Formulas for Intermediate and Far Fields

In all cases, Near-Field and Intermediate-Field formulas are evaluated in panel coordinates. For the vorticity effects discussed in this section the Far-Field formulas are also evaluated in panel coordinates by truncating the Intermediate-Field expansions with the first terms. The ranges of distance from the panel origin where the various formulas are used remains unchanged.

Thus the superscript zero components are evaluated using expansions (70) for the source velocities (61).

Also, superscript one components are evaluated using expansions (85), together with (87) and

$$
\begin{aligned}
J^*_1 &= x\phi^*_{10} - \phi^*_{20} \\
J^*_2 &= y\phi^*_{10} - \phi^*_{11} \\
J^*_3 &= x\phi^*_{01} - \phi^*_{11} \\
J^*_4 &= y\phi^*_{01} - \phi^*_{02}
\end{aligned}
\tag{151}
$$

In an exception to the above-stated rule, expansion (85) retains two terms in the Far-Field if $p + q = 1$. This is to ensure that expansions are terminated with area moments of even order.

For the superscript two components, equations (150) are used with θ_{mn} from equation (106) with $V_{\omega R}$ from (108) and with (149) replaced by

$$
\begin{aligned}
w_{xz} &= -xV_{\omega R} + 3z(P\theta_{30} + 2Q\theta_{21} + R\theta_{12}) \\
w_{yz} &= -yV_{\omega R} + 3z(P\theta_{21} + 2Q\theta_{12} + R\theta_{03})
\end{aligned}
\tag{152}
$$

In equation (106b) both terms are retained in the Far-Field for the reason stated above.

9.2.3 Changes in the Formulas Needed to Obtain the Effect of a Wake Panel

The wake is characterized by the fact that the equivalent dipole distribution is constant along N-lines. This necessitates changes in the basic assembly formulas (145), (147) and (150). However, the formulas for the individual quantities appearing in these equations in the Near-, Intermediate-, and Far-Fields are unchanged.

The total arc length of an N-line from lower-surface trailing edge to upper-surface trailing edge is denoted L (total) in reference 1 and given by equation (7.9.2). This quantity, evaluated on the first and second N-lines of the panel, is used in the wake formulas.

Equations (145) are replaced by

$$
\begin{aligned}
V_{\omega x}^{(0)}(S) &= 0 \\
V_{\omega x}^{(0)}(F) &= 0 \\
V_{\omega y}^{(0)}(S) &= (145) \text{ with } h_S \text{ replaced by } L_S \text{ (total)} \\
V_{\omega y}^{(0)}(F) &= (145) \text{ with } h_F \text{ replaced by } L_F \text{ (total)} \\
V_{\omega z}^{(0)}(S) &= -\left[\frac{L_S \text{ (total)}}{w} - c(n_1 + n_3)\right] V_y \text{ (source)} \\
V_{\omega z}^{(0)}(F) &= \left[\frac{L_F \text{ (total)}}{w} - c(n_1 + n_3)\right] V_y \text{ (source)}
\end{aligned}
\tag{153}
$$

Equations (147) are replaced by

$$
\begin{aligned}
V_{\omega x}^{(1)}(S) &= 2\left[\frac{L_S \text{ (total)}}{w} - c(n_1 + n_3)\right](PJ_2^* + QJ_4^*) \\
V_{\omega x}^{(1)}(F) &= -2\left[\frac{L_F \text{ (total)}}{w} - c(n_1 + n_3)\right](PJ_2^* + QJ_4^*) \\
V_{\omega y}^{(1)}(S) &= 2c\phi_{01} - \left[\frac{L_S}{w} - c(n_1 + n_3)\right](H + 2PJ_1^* + 2QJ_3^*) \\
V_{\omega y}^{(1)}(F) &= -2c\phi_{01} + \left[\frac{L_F}{w} - c(n_1 + n_3)\right](H + 2PJ_1^* + 2QJ_3^*)
\end{aligned}
\tag{154}
$$

$$V_{\omega z}^{(1)}(S) = -2cJ_4^* \qquad (154)$$

$$V_{\omega z}^{(1)}(F) = +2cJ_4^*$$

Equations (150) are replaced by

$$V_{\omega x}^{(2)}(S) = 0$$

$$V_{\omega x}^{(2)}(F) = 0$$

$$V_{\omega y}^{(2)}(S) = \text{unchanged with } h_S \text{ replaced by } L_S \text{ (total)} \qquad (155)$$

$$V_{\omega y}^{(2)}(F) = \text{unchanged with } h_F \text{ replaced by } L_F \text{ (total)}$$

$$V_{\omega z}^{(2)}(S) = \left[\frac{L_S \text{ (total)}}{w} - c(\eta_1 + \eta_3)\right] w_{yz}$$

$$V_{\omega z}^{(2)}(F) = -\left[\frac{L_F \text{ (total)}}{w} - c(\eta_1 + \eta_3)\right] w_{yz}$$

The option exists to make the last panel of the wake semi-infinite in the manner of reference 1.

9.3 Modification for Parabolic Chordwise Vorticity Variation

As discussed in reference 5, the assumption of constant vorticity around a wing section can lead to numerical difficulties on certain wings with very thin trailing edges. Accordingly, a second chordwise variation option is required. The important consideration is to have the "bound" vorticity strength approach zero at the trailing edge on both upper and lower wing surfaces. This is accomplished by a quadratic global variation of vorticity as a function of arc length along an N-line. While only two global chordwise variations have been incorporated into the present method, many such variations are possible. If in the future numerical difficulties should be encountered for certain types of geometry, say, for example, a wing that is very thin over its entire length, a properly chosen chordwise vorticity variation could eliminate these difficulties. Moreover, as will be seen below, the required modifications to the program are quite minor. This flexibility is due to the use of vorticity as an auxiliary singularity.

To implement the parabolic vorticity option, the linear variation of the equivalent dipole strength along an N-line (138) is replaced by a cubic variation having zero derivative at the upper and lower trailing edge. Specifically, (138) is replaced by

$$\mu = Bs\left\{3\,\frac{s}{L\ (\text{total})} - 2\left[\frac{s}{L\ (\text{total})}\right]^2\right\} \tag{156}$$

where all symbols have the same meaning as in section 9.2. The above is a global variation. The variation over an individual panel can be no higher a degree than quadratic, and in the initial version of the present method has been taken as linear. It is assumed that the dipole distribution on a panel agrees with (156) at the corners of the panel and varies linearly in between. Thus, the overall behavior is that of an inscribed-polygon approximation to (156).

For an individual panel the arc length measured along an N-line from the trailing edge to the lower corner of the panel is L (equation (7.2.23) of reference 1), while the arc length associated with the upper corner is $L + d$ (equation (7.2.22) of reference 1). Both L and d are subscripted with F or S to denote, respectively, the first or second N-lines. The linear function that agrees with (145) at these two values of arc length is

$$\mu = B(H + I\xi) \tag{157}$$

where on the two N-lines the constants H and I have the values

$$H_F = \frac{3}{L_F\ (\text{total})}\,(h_F^2 - \xi_1\xi_2) - \frac{2}{[L_F\ (\text{total})]^2}\,[h_F^3 - \xi_1\xi_2(3h_F + \xi_1 + \xi_2)]$$

$$I_F = \frac{3}{L_F\ (\text{total})}\,(2h_F + \xi_1 + \xi_2) - \frac{2}{[L_F\ (\text{total})]^2}\,[3h_F^2 + 3h_F(\xi_1 + \xi_2) + \xi_1^2 + \xi_2^2 + \xi_1\xi_2] \tag{158}$$

$$H_S = \frac{3}{L_S\ (\text{total})}\,(h_S^2 - \xi_3\xi_4) - \frac{2}{[L_S\ (\text{total})]^2}\,[h_S^3 - \xi_3\xi_4(3h_S + \xi_3 + \xi_4)]$$

$$I_S = \frac{3}{L_S\ (\text{total})}\,(2h_S + \xi_3 + \xi_4) - \frac{2}{[L_S\ (\text{total})]^2}\,[3h_S^2 + 3h_S(\xi_3 + \xi_4) + \xi_3^2 + \xi_4^2 + \xi_3\xi_4]$$

where all symbols have the same meaning as in section 9.2. Thus the quadratic form (140) for the variation of dipole strength over a panel is replaced by

$$\mu = \frac{B_F I_F - B_S I_S}{W}\xi\eta + \frac{B_F H_F - B_S H_S}{W}\eta + \frac{B_S I_S \eta_1 - B_F I_F \eta_3}{W}\xi + \frac{B_S H_S \eta_1 - B_F H_F \eta_3}{W}$$

$$+ c(B_F - B_S)(\eta - \eta_3)(\eta - \eta_1) + d(B_F - B_S)\xi^2 \qquad (159)$$

where in the initial version of the present method c and d are set equal to zero. The dipole derivative formulas (141) are modified in an obvious way.

Thus the elaborate vorticity velocity formulas of section 9.2 are modified to account for parabolic vorticity variation by the following procedure:

a. Terms containing c or d are not changed.

b. In terms containing h_F or h_S these quantities are replaced by H_F or H_S, respectively

c. All other terms are multiplied by I_F or I_S as appropriate.

In the constant chordwise vorticity option, the parameter c is nonzero on wake panels if the "piecewise linear" spanwise variation of vorticity is used (section 7.9 of reference 1). However, if the parabolic chordwise vorticity option is used, c is taken as zero on all panels.

9.4 The Piecewise Linear Spanwise Vorticity Variation

The third aspect of the global vorticity algorithm is the variation from N-line to N-line across the "span" of a panel. The base method of reference 1 has two options: constant and linear. In the former the equivalent dipole strength is discontinuous across an N-line by an amount equal to the product of the spanwise gradient and the panel width. Concentrated trailing vortex filaments of this strength lie along the N-line. This representation is inconsistent with a higher-order formulation and has been excluded from the vorticity velocity formulas of section 6.3. Accordingly, the present method has only one type of spanwise variation, the linear one.

Once the vorticity velocities $\vec{V}_\omega(F)$ and $\vec{V}_\omega(R)$ have been calculated by the procedures of sections 9.1, 9.2 and 9.3, they may be used in exactly the same way as the corresponding quantities of the base method. Thus the

procedure of section 7.11 of reference 1 may be used without change to generate the vorticity onset flows that are used to satisfy the Kutta condition.

10.0 THE KUTTA CONDITION

The Kutta condition is applied in one of two ways: a condition of flow tangency in the wake or a condition of pressure equality on the upper and lower surfaces of the trailing edge, which amounts to a condition of equal velocity magnitude, (section 7.13, reference 1). The wake tangency condition is applied in exactly the same manner as reference 1. This section is concerned with the equal-pressure condition, which uses a different iterative procedure from that of reference 1.

As a numerical approximation, the Kutta condition may be applied by equating pressures at the control points of the two panels adjacent to the trailing edge on the upper and lower surfaces of the wing. Alternatively, velocities at the upper surface control points of the few panels nearest the trailing edge could be extrapolated to obtain velocity components "at" the trailing edge upper surface, and the same could be done for the lower surface. This last would allow application of the Kutta condition more nearly at the trailing edge, and the analogy of this procedure yields considerable improvement in accuracy in two-dimensional cases. However, in the initial version of the present method, pressure equality is applied at the control points of the adjacent panels.

However the point of application of the Kutta condition is chosen, the logic of the calculation is the same. In particular, a velocity vector can be calculated at the upper and at the lower trailing edge point for each strip of panels (figure 1) and for each onset flow — both the uniform stream and the several vorticity onset flows (section 9.4). It is necessary to introduce some notation. A subscript m denotes quantities associated with the m-th lifting strip of panels, and $m = 1, 2, \ldots, L$, where L is the total number of lifting strips. Superscript ∞ denotes velocities obtained in the flow solution for a uniform onset flow, and superscript $k = 1, 2, \ldots, L$ denotes velocities obtained in the flow solution due to the vorticity onset flow associated with the K-th lifting strip. $B^{(k)}$ denotes the unknown multiplicative constant to be applied to the vorticity solution corresponding to the k-th lifting strip. Finally, (Up) or (Lo) denote velocities at the upper or lower trailing-edge point, respectively. Thus the velocity vectors at the trailing-edge points of the m-th strip are

$$\vec{V}_m(Up) = \vec{V}_m^{(\infty)}(Up) + \sum_{k=1}^{L} B^{(k)} \vec{V}_m^{(k)}(Up)$$

$$m = 1, 2, \ldots, L \quad (160)$$

$$\vec{V}_m(Lo) = \vec{V}_m^{(\infty)}(Lo) + \sum_{k=1}^{L} B^{(k)} \vec{V}_m^{(k)}(Lo)$$

These are analogous to the velocity vectors (7.13.3) of reference 1. A unit vector for each strip of panels is defined by

$$\vec{V}_m(Avg) = \frac{\vec{V}_m(Up) + \vec{V}_m(Lo)}{|\vec{V}_m(Up) + \vec{V}_m(Lo)|} \qquad m = 1, 2, \ldots, L \quad (161)$$

The condition that the velocity vectors at the upper and lower trailing-edge points of each strip have equal magnitudes may be written

$$\vec{V}_m(Up) \cdot \vec{V}_m(Avg) = \vec{V}_m(Lo) \cdot \vec{V}_m(Avg) \qquad m = 1, 2, \ldots, L \quad (162)$$

Equations (162) consist of L simultaneous quadratic equations for the L unknowns $B^{(k)}$. All coefficients of equations (162) can be expressed in terms of the $2m(m + 1)$ individual velocities appearing in (160). Equations (162) are solved iteratively beginning with $B^{(k)} = 0$. At any stage of the iteration the $\vec{V}_m(Avg)$ are evaluated from the currently known set of $B^{(k)}$. These are used in (162) to obtain an $L \times L$ set of <u>linear</u> equations for the successive set of $B^{(k)}$. The iteration has been thoroughly tested in the base method of reference 1 and has converged very rapidly in all cases.

11.0 CALCULATED RESULTS

To illustrate the improvements that the higher-order method of this report has been able to effect compared to the base method of references 1 and 2, a number of cases have been run for which high-accuracy solutions are available. While it would undoubtedly be useful to run more such cases, the results presented below strongly indicate the effectiveness of the present method, even in its initial form.

The triaxial ellipsoid is the only truly three-dimensional body for which an analytic solution exists. A geometry was selected having semiaxes equal to 1, 2 and ½ in the x, y, and z directions, respectively, as shown in the sketch of figure 6. Calculations were performed for two uniform onset flows — one parallel to the x-axis and one to the z-axis — using 16 strips of panels defined by section cuts (N-lines) at constant values of y from +2 to -2. Each strip had 30 panels around the elliptical cross-section — a total of 480 effective panels (symmetry was employed). Calculated and analytic surface velocities along the curve in the xz-plane are compared in figure 6. As pointed out in references 5, 6 and 7, the base method enjoys a certain amount of cancellation of errors when calculating flow about smooth convex shapes. Thus the higher-order procedure cannot be expected to yield consistent gains in accuracy for such cases. In view of this, the small but definite improvement in accuracy exhibited by the higher-order results in figure 6 is quite significant.

Greater gains in calculational accuracy can be realized by the higher-order method when the body has concave regions. The geometry selected is the circular nacelle shown in the sketch of figure 7. With the onset flow parallel to the axis of symmetry, the total flow is axisymmetric and a high-accuracy, graphically exact solution can be obtained by the method of reference 6. Nevertheless, this is a meaningful case for comparing the three-dimensional base and higher-order methods, because they do not take advantage of the axial symmetry but panel the nacelle both axially and circumferentially. The three-dimensional results shown in figure 7 were obtained using a distribution of 17 panels axially on the inner surface of the nacelle and the same number on the upper surface. Circumferentially, 18 effective panels were employed, so that each panel subtends an angle of 20°. This is a lifting case. Kutta

conditions are applied along the trailing edge of the nacelle, and the vorticities on the strips are adjusted accordingly. Because the axisymmetric solution of reference 6 employed a much larger number of panels axially than either of the three-dimensional methods, it applied the Kutta condition of equal upper and lower surface pressures at a point nearer the true trailing edge. This disturbs the agreement in the trailing-edge region, but has relatively little effect at forward locations. Two-dimensional experience indicates that this situation can be alleviated either by extrapolating the Kutta condition to the trailing edge or by using small panels adjacent to the trailing edge. Figure 7 dramatically illustrates the effect of concavity on the exterior surface, where the body is convex, all three calculated solutions agree quite well (away from the trailing edge). On the concave interior surface the lower order method of reference 1 gives results that are seriously in error, while the higher-order method of the present report agrees with the high-accuracy solution almost exactly.

The most impressive improvements in accuracy due to inclusion of higher-order effects occur in interior flows. To illustrate this, the geometry selected is the circular duct of area ratio four shown in figure 8. The duct was paneled using strips of panels around the circular cross sections. Each strip of panels has a width equal to one-third of the maximum duct radius — a total of 42 strips along the length of the duct. Each strip contains 18 effective panels (symmetry is employed) around the circular cross sections, so that each panel subtends an angle of 20^{o}. For purposes of comparison, a high accuracy, graphically exact solution for the duct has been obtained by using the higher-order axisymmetric method of reference 6. Several calculations have been made, each with twice as many panels along the duct as the previous calculation. This study has verified that the solution obtained by the higher-order axisymmetric program using 140 panels along the duct may be considered graphically exact, and accordingly it is used as a standard of comparison in figure 8. The results of three different three-dimensional calculations are compared with the high accuracy solution in figure 8. The first two use the 42 x 18 panel distribution described above — a total of 756 effective panels. One calculation was performed with the higher-order method of the present report and one with the base method of references 1 and 2. The base-method solution is so inaccurate as to be unusable, while the higher-order solution is scarcely distinguishable from the exact. To

provide another standard of judgment, the results of two base-method calculations using a greatly increased panel number are also shown in figure 8. These cases, which have been taken from reference 2, each use 4200 effective panels. One has 42 strips of panels along the duct, each with 100 panels around the circular cross section. The other has 84 strips of panels along the duct, each with 50 panels around the circular cross section. The calculated surface velocities for both cases agree fairly well (reference 2), and so they are shown as a single curve in figure 8. Even with this greatly increased panel number, the errors in the base-method calculation are an order of magnitude larger than those of the higher-order calculation. Since approximately 5.5 times as many panels are employed, the computing time for the large panel number case of figure 8 is at least 20 times larger than that of the higher-order method. Thus, for the duct of figure 8, the higher-order method obtained a factor 10 increase in accuracy and a factor 20 decrease in computing time.

12.0 PRINCIPAL NOTATION

A,B	coefficients of linear terms in the expression for local surface shape, equation (110)
$\vec{n}$	unit normal vector with components n_ξ, n_η, n_ζ
P,Q,R	coefficients of quadratic terms in the expression for local surface shape, equations (6) or (110). These "local curvatures" are fundamental to the higher-order procedure.
r	distance between a field point (x,y,z) and a point (ξ,η,ζ) on the curved panel
r_f	distance between a field point (x,y,z) and a point $(\xi,\eta,0)$ on the projected flat panel
r_o	distance from a field point (x,y,z) to the control point of a curved panel
t	panel dimension. Usually the maximum chord of the projected flat panel.
V	fluid velocity. Used with various subscripts and superscripts to denote components and velocities due to various effects.
x,y,z	Cartesian coordinates of a point in space, usually in the panel coordinate system. Used as subscripts to denote partial derivatives and components of vectors.
ζ_2	the summed quadratic terms of the local shape, equation (6). Subscripts denote derivatives.
μ	dipole strength. Used with various subscripts to denote derivatives at the origin of panel coordinates
ξ,η,ζ	Cartesian coordinates of a point on the curved panel in its own coordinate system. ξ and η denote coordinates of a point on the projected flat panel. Used as subscripts to denote derivatives and vector components.
σ	source density. Used with various subscripts to denote derivatives at the origin of panel coordinates.

ϕ velocity potential. Used with various subscripts and superscripts to denote potentials due to various effects.

$\vec{\omega}$ vorticity strength

Note: The equations of this report are not intended to stand independent of those of reference 1. Similarly, quantities defined there are not repeated here. These include: I_{mn}, ϕ_{mn}, J_{mn}, u (with various subscripts), m_{32}, b_{32}, B, L, w, h, a_{mn}, ξ_K, η_K and subscripts F and S.

13.0 REFERENCES

1. Hess, J.L.: Calculation of Potential Flow about Arbitrary Three-Dimensional Lifting Bodies. McDonnell Douglas Report No. MDC J5679-01, October 1972. (A somewhat condensed version is contained in Computer Methods in Applied Mechanics and Engineering, Vol. 4, No. 3, November 1974.)

2. Hess, J.L. and Smith, A.M.O.: Calculation of Nonlifting Potential Flow about Arbitrary Three-Dimensional Bodies. Journal of Ship Research, Vol. 8, No. 2, 22 (Sept. 1964). (A somewhat expanded version is contained in Douglas Aircraft Report No. ES 40622, March 1962.)

3. Halsey, N.D. and Hess, J.L.: A Geometry Package for Generation of Input Data for a Three-Dimensional Potential Flow Program. NASA CR 2962, June 1978.

4. Halsey, N.D.: A Three-Dimensional Potential-Flow Program with a Geometry Package for Input Data Generation. NASA CR 145311, March 1978.

5. Hess, J.L.: Higher-Order Numerical Solution of the Integral Equation for the Two-Dimensional Neumann Problem. Computer Methods in Applied Mechanics and Engineering, Vol. 2, No. 1, February 1973.

6. Hess, J.L.: Improved Solution for Potential Flow about Arbitrary Axi-symmetric Bodies by Use of a Higher-Order Surface-Source Method. Computer Methods in Applied Mechanics and Engineering, Vol. 5, No. 3, May 1975.

7. Hess, J.L.: The Use of Higher-Order Surface Singularity Distributions to Obtain Improved Potential-Flow Solutions for Two-Dimensional Lifting Airfoils. Computer Methods in Applied Mechanics and Engineering, Vol. 5, No. 1, February 1975.

8. Hess, J.L.: Consistent Velocity and Potential Expansions for Higher-Order Singularity Methods. McDonnell Douglas Report No. MDC J6911, June 1975. (Superceded by present report.)

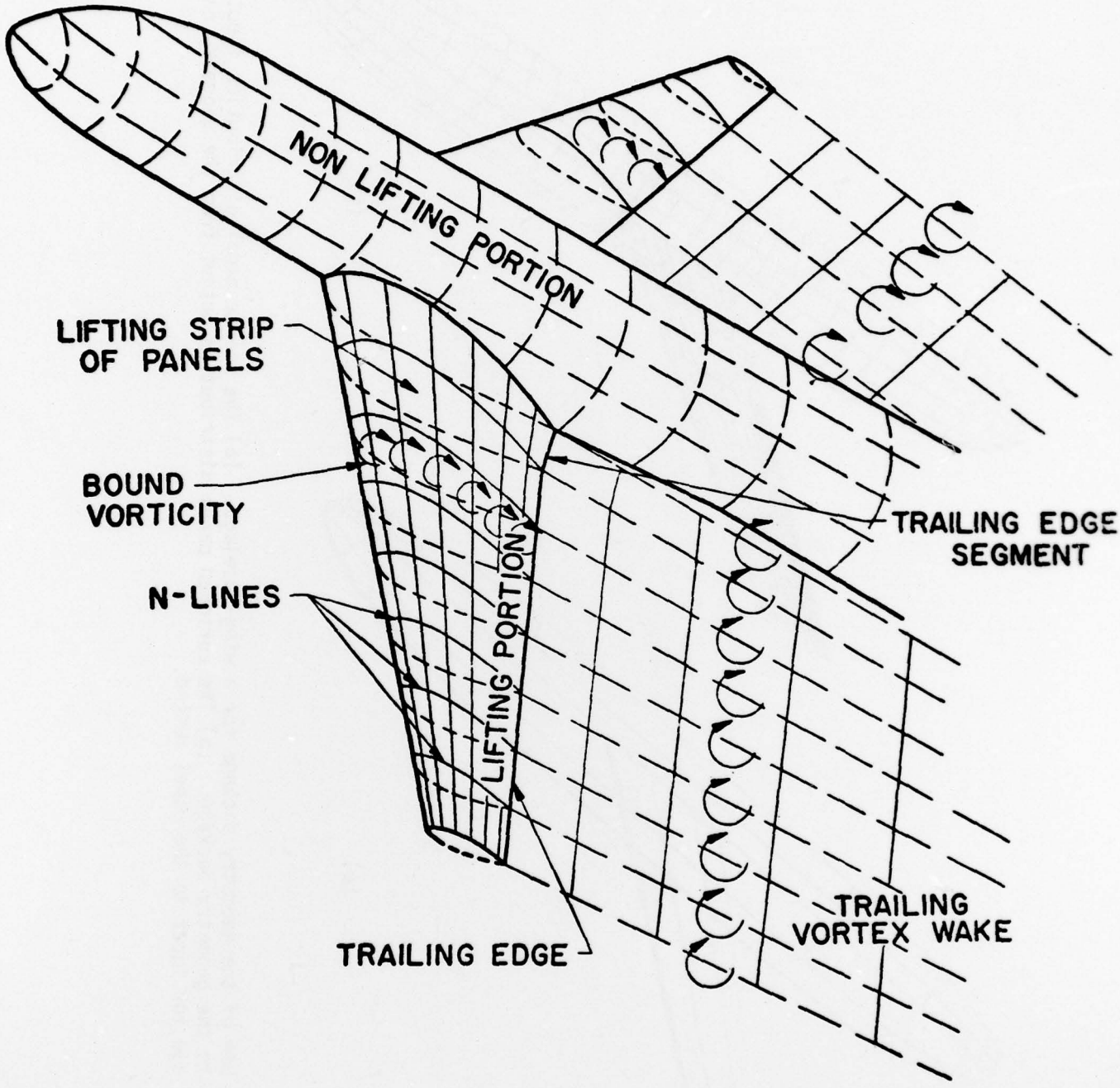

Figure 1. Representation of a three-dimensional lifting configuration.

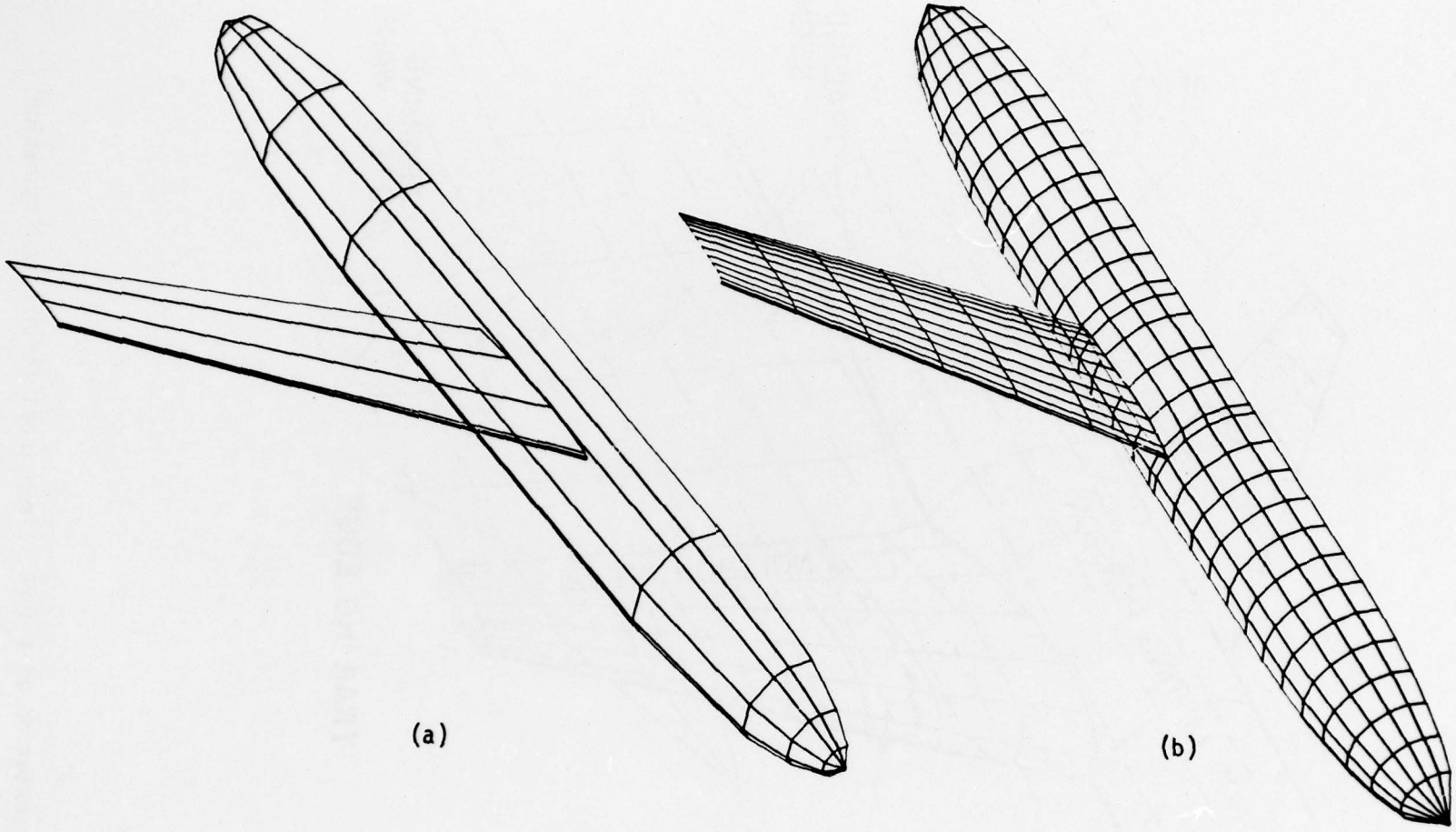

Figure 2. Use of the geometry package for a wing-fuselage. (a) The sparse panel distribution input to the geometry package. (b) The enriched panel distribution output from the geometry package for input to the panel method.

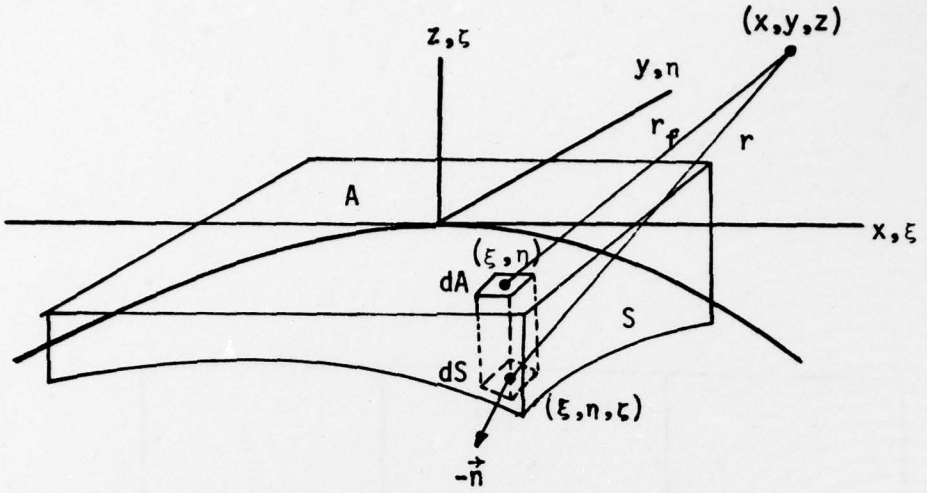

Figure 3. A general curved surface panel and its projection in the tangent plane.

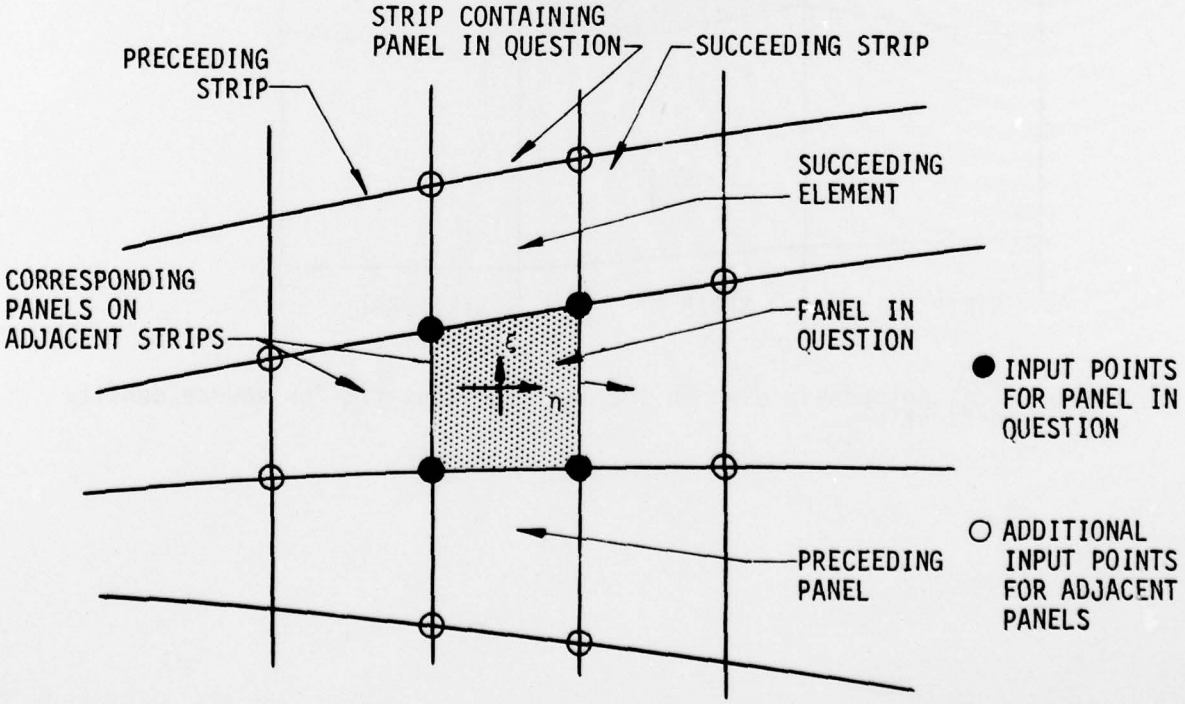

Figure 4. The input points of adjacent panels used to compute local surface curvatures.

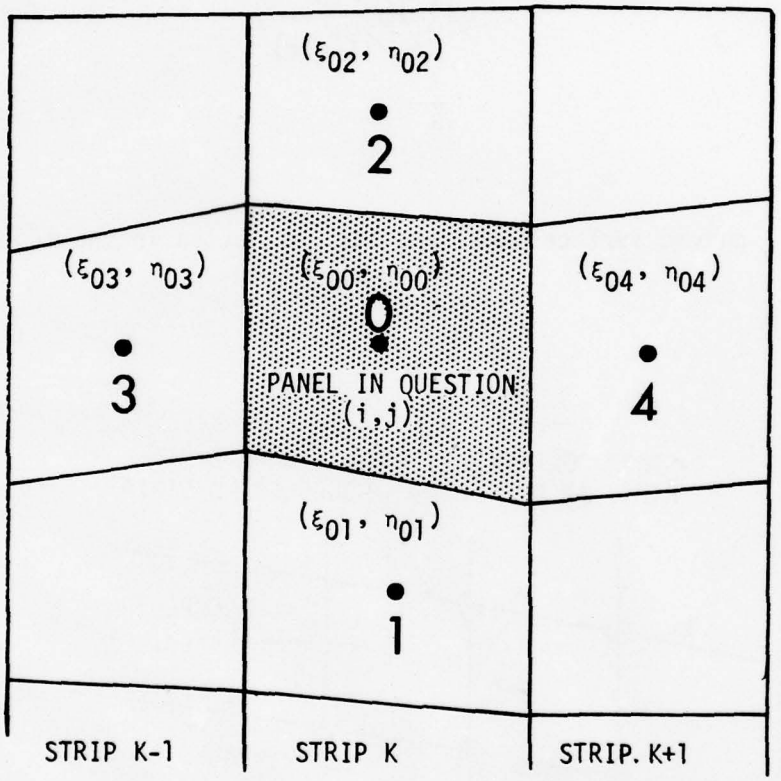

Figure 5. Adjacent panels used in the least-squares fit for source density derivatives.

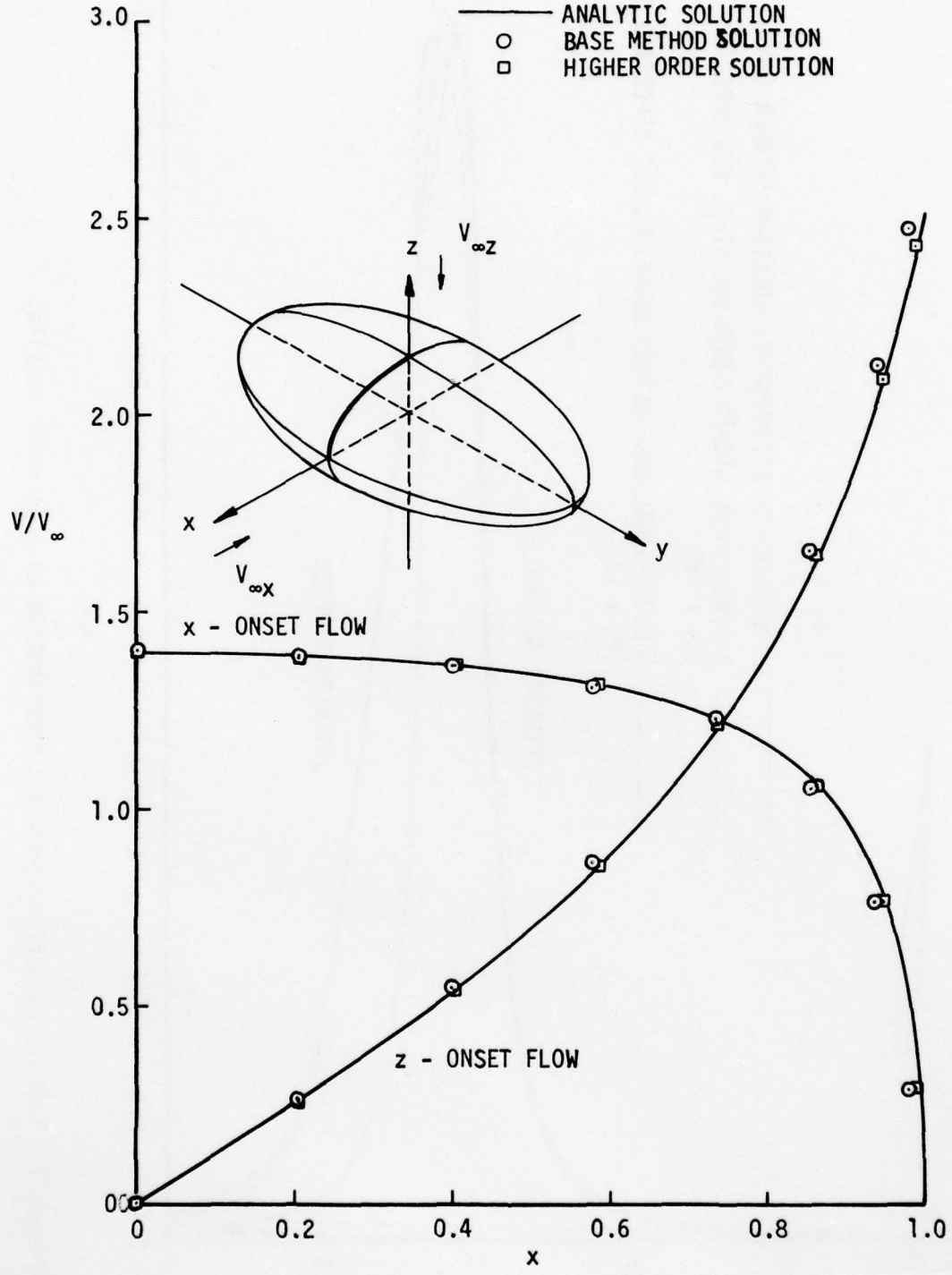

Figure 6. Comparison of calculated and analytic surface velocities on a triaxial ellipsoid with axes ratios 1, 2, 1/2 in the x,y,z directions. Velocities shown are along the curve lying in the xz-plane.

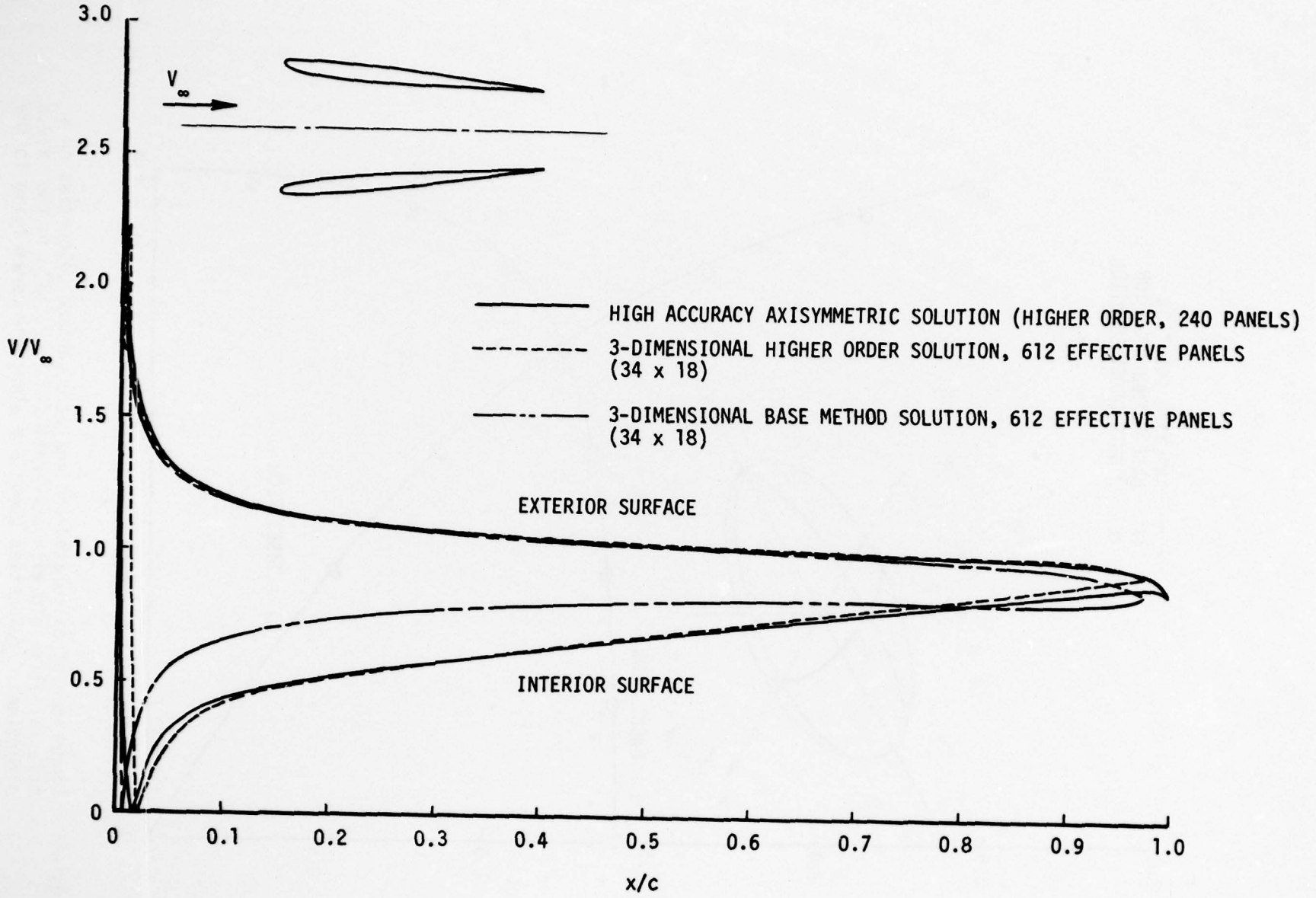

Figure 7. Calculated surface pressure distribution on a circular nacelle.

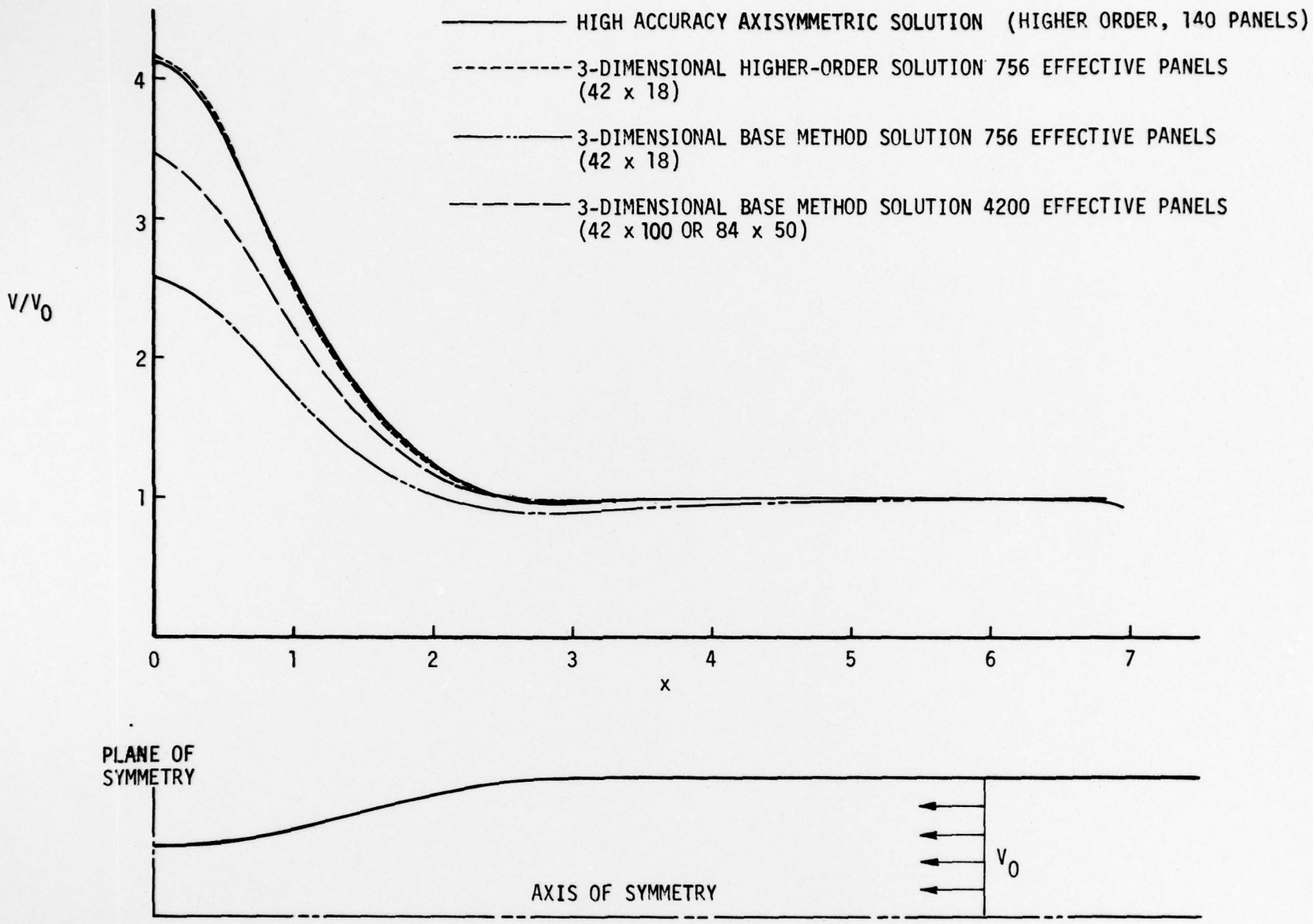

Figure 8. Calculated surface velocity distributions on a circular duct of area ratio four.